Master of Science Thesis

Optimization for automatic whole brain volumetry: An MPRAGE image contrast study of a 12- and 32 channel head coil at 3T

Love Nordin

Supervisor: Terri Lindholm, PhD

This work has been performed at the Department of Diagnostic Medical Physics and the SMILE Image Laboratory Karolinska University Hospital Huddinge

Medical Radiation Physics
Clinical Sciences, Lund
Lund University, 2009

ABSTRACT

Introduction: Regional and global brain volumes are of great interest in many different research projects, not least in Alzheimer's research. The purpose of this project is to optimize the MPRAGE sequence for automatic and repeatable segmentation of human brain tissue. The volume is calculated for the whole brain, white matter (WM), grey matter (GM) and cerebrospinal fluid (CSF). **Materials and methods:** MPRAGE (Magnetization Prepared Rapid Acquisition by Gradient Echo) is a T1 weighted 3D sequence with high resolution showing fine anatomical details of the brain. The high resolution and high T1 contrast makes it a good choice for tissue specific segmentation of the brain. Parameters in the sequence that are altered to manipulate the contrast relationships between WM/GM and GM/CSF are flip angle (FA) and inversion time (TI). FA of 8-11° are used for TI varying between 700-1000 ms. The contrast relationship between different types of tissue is an important factor to achieve a successful segmentation. The project includes a volunteer study with 9 healthy subjects aged 22-41 (5 men and 4 women) and is carried out on a 3T Magnetom Trio (Siemens, Medical Solution, Erlangen, Germany). The study also contains a comparison between a 12 channel and a 32 channel Matrix head coil and a test of repeatability of the optimized sequence. Brain Map Statistics is a locally developed software used for fully automatic brain tissue segmentation. The image histograms are analyzed for quantification and classification of brain tissue. The images are also evaluated by an experienced neuro-radiologist in terms of tissue contrast for clinical diagnosis. **Results:** Contrast differences between WM-GM up to 56% could be found when the contrast parameters of the sequence were changed. It is shown that small FA and short TI results in higher WM-GM contrast. The best contrast parameters were found to be TI = 850 ms and FA = 8° from the optimization. All images acquired with FA and TI in the range of 8-10° and 800-900 ms respectively was approved for clinical use. The repeatability study resulted in a coefficient of variation $\leq 0.7\%$ for the total brain volume and BPF with both coils. **Conclusions:** No other studies about optimization of the MPRAGE sequence, also containing a comparison between two different multi channel coils has been found. The comparison between the 12- and the 32 channel coils show that the contrast variation as a function of FA and TI is larger with the 32 channel coil. This indicates that the 32 channel coil is in a bigger need of optimization. The anatomical details were slightly better with the 32 channel coil when small FA and short TI were used. The relative contrast between WM-GM and GM-CSF was higher for the 12 channel coil. The repeatability result needs further investigation since the coefficient of variation is smaller in a previous study on a 1.5 T MRI unit.

Keywords: MPRAGE, automatic segmentation, 3T, contrast parameter, volumetry, 12 vs. 32 channel.

CONTENTS

1 INTRODUCTION

With an increasing average age of many populations, dementia is becoming a public health problem. The most common form of dementia is Alzheimer's disease which is associated with progressive cerebral atrophy. Mild cognitive impairment (MCI) is a translational state between the changes of normal aging and early dementia. MCI can be considered as a risk factor for developing Alzheimer's disease [1, 2].

In order to track these neurodegenerative diseases at an early stage, a reliable and repeatable method for volumetric measurements of brain tissue is needed. An accurate understanding of how brain changes in normal aging differ from those in dementia is required [3]. MRI is an excellent tool for this purpose since it has a superior soft tissue contrast compared to other imaging methods. MPRAGE is a 3D MRI sequence used for segmentation of brain tissue and volumetric measurements. The MPRAGE sequence has high signal intensity and good grey-white matter contrast. In order to get successful segmentation results the MPRAGE sequence needs to be optimized in terms of tissue contrast. The optimization of the MPRAGE sequence is performed at a 3T Magnetom Trio (Siemens, Medical Solution, Erlangen, Germany). The optimization is carried out both for a 12 channel head coil and a 32 channel head coil separately. The 32 channel coil has a higher SNR than the 12 channel coil. The results are compared between both coils and the differences are evaluated.

The images should not only have maximized contrast relationship between white matter (WM), grey matter (GM) and cerebrospinal fluid (CSF), but they should also be satisfactory to the radiologists in terms of tissue contrast from a clinical point of view. This requires that the MPRAGE sequence is optimized for a tissue segmentation purpose, and still has clinical diagnostic value. The optimization is carried out by varying the parameters of the sequence that affect signal intensity and image contrast. A group of 9 volunteers was used to perform the optimization. After the sequence had been optimized for tissue contrast, the repeatability was tested on one volunteer by conducting multiple scans using this optimized sequence.

Manual segmentation of the brain is very time consuming, and the result can vary depending on the operator. A fully automatic segmentation tool is used in this study to get a fast and objective result.

2 BACKGROUND

2.1 The MPRAGE sequence

Some basic requirements for structural brain imaging is that the resolution should be high (~1 mm), there should be high contrast between WM/GM and GM/CSF and finally the acquisition time should not be too long [4]. MPRAGE, which is an abbreviation for Magnetization Prepared Rapid Acquisition by Gradient Echo, is a 3D gradient echo based sequence which is well suited for this purpose. MPRAGE generates T1 weighted images with very high resolution and good anatomical detail (see example in figure 1). Another benefit is the use of small flip angles (typically in the range of 8-9º) which results in a low specific absorption rate (SAR), even when working with high field MRI (≥3T).

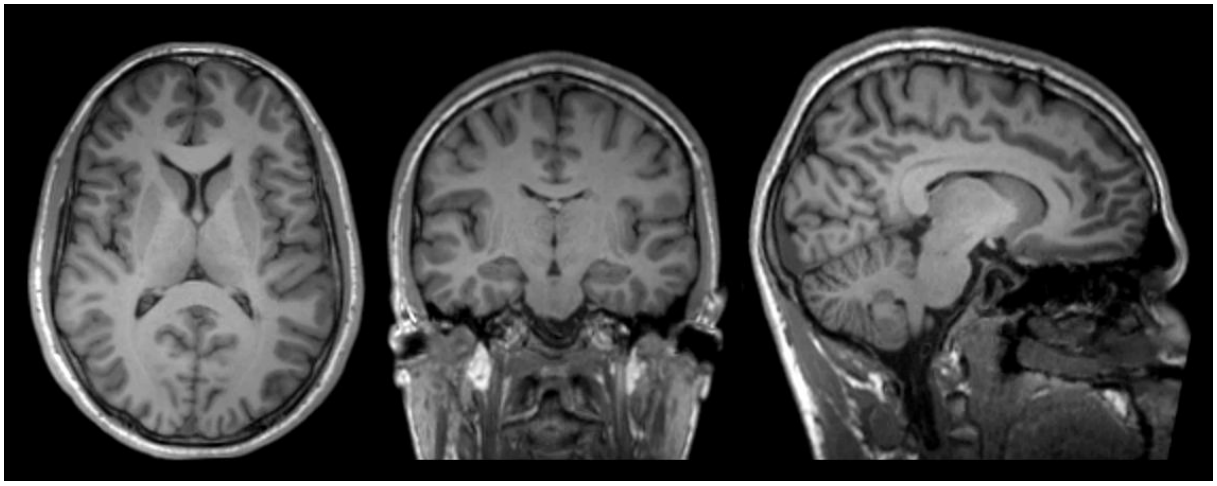

Figure 1. Example of different cross sections of MPRAGE images with a 32 channel head coil at a 3T MRI unit.

In 3D imaging there are two different phase encoding directions. It is not possible to acquire the whole of 3D k-space from a single preparation because of the large amount of combinations among these two phase encoding directions. Instead, all slice-lines of data are acquired from each preparation as shown in figure 2. After each slice a recovery delay time (TD) takes place before moving on to the next in-plane line of k-space. As a consequence of TD all the data is acquired with the same degree of relaxation [5]. TD, which is typically around 300 ms, adds considerably to the total acquisition time.

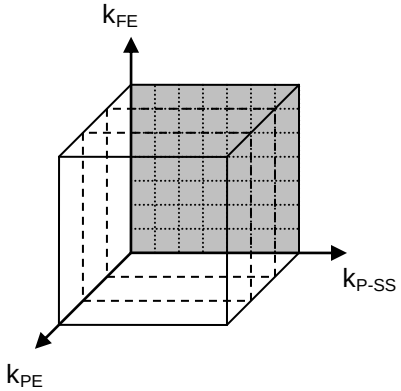

Figure 2. K-space encoding. All slice selection lines ($k_{P\text{-}SS}$) are acquired along with the frequency encoding steps (K_{FE}) from each preparation. This part of the sequence is repeated once for each phase encoding step (k_{PE}).

The MPRAGE sequence begins with a 180° inversion pulse which is followed by an inversion time (TI). After TI, follows a gradient spoiler in the slice selection direction to prevent unwanted FID (Free Induction Decay) from forming, this may otherwise lead to image artefacts and wrong contrast conditions. Different phase encoded signals from different excitations may lead to banding artefacts [5].

In the RAGE loop (the grey area in figure 3) a RF excitation pulse, α, is applied with a random phase angle. The point of doing this is to reduce T_2 by dephasing of the spins which reduces the remains of the transverse magnetization from previous excitations [5]. In the RAGE loop, one entire slice is encoded. $N_{PE(SS)}$ is the number of phase encoding steps in the slice selection direction. The duration of each loop is given by the repetition time (TR). The RAGE loop itself is repeated once for each phase encoding step ($N_{PE(PE)}$ times), starting with the inversion pulse. The echo time (TE) is the time between α and MR signal sampling, corresponding to maximum of the echo.

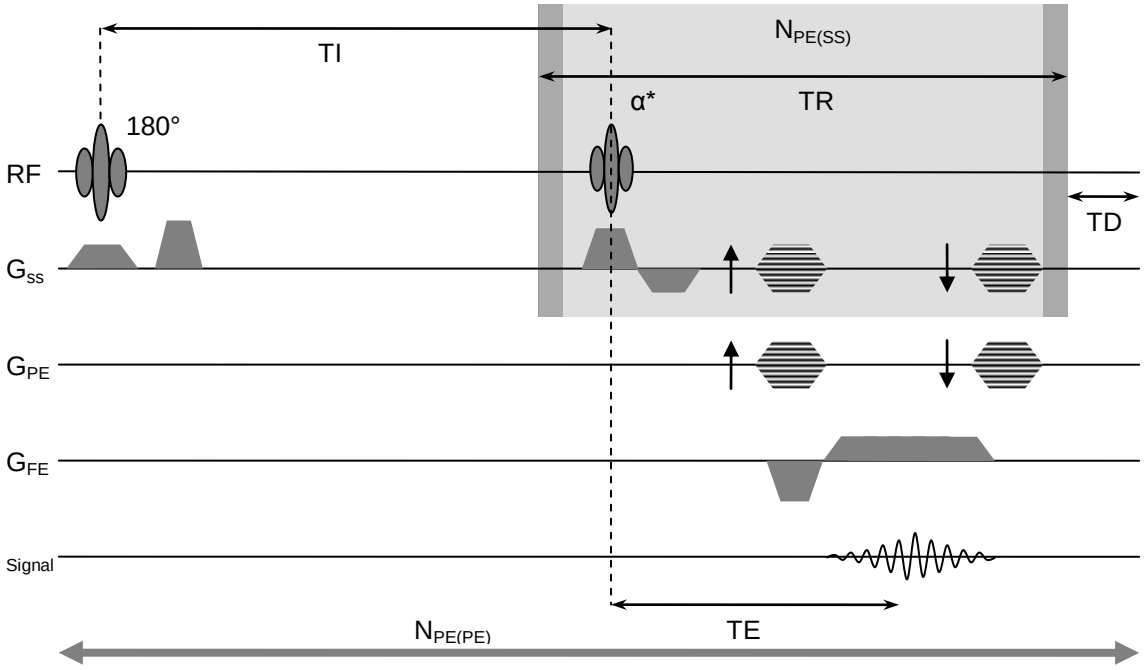

Figure 3. MPRAGE sequence. The RAGE loop of duration TR shown in the grey area recur $N_{PE(SS)}$ times until all phase encoding steps in the slice selection direction are encoded. The loop itself is repeated $N_{PE(PE)}$ times, once for each phase encoding step.

Both the slice encoding gradient and the phase encoding gradient are rewound after each inversion pulse and each RF pulse. This means that the phase of the transverse magnetization is reset to zero by reversing the sign of the gradient pulses after the data acquisition period [5].

The sequence starts with a 180º inversion pulse to maximize the T_1 contrast which is reached after a delay time, TI. This is shown for tissue A and B in figure 4 and the following example.

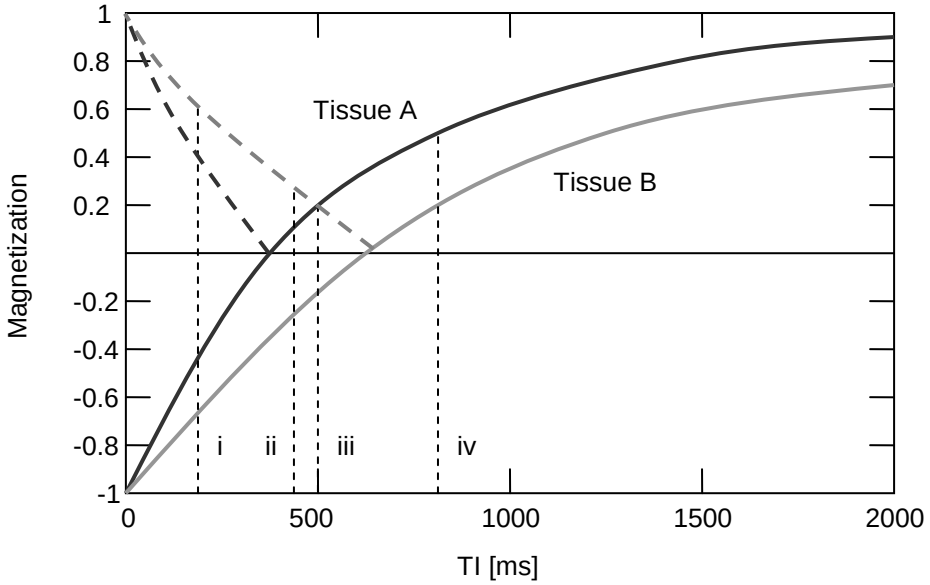

Figure 4. Signal intensity as a function of TI for tissue A (dark grey) and B (light grey). The dotted lines show the measured magnetization since it is the absolute value of the magnetization that generates the signal.

Example
Tissue A has shorter T1 relaxation time than tissue B. At TI = 0, just when the inversion pulse has taken place, the signal from Tissue A and B has the same amplitude assuming both have the same equilibrium magnetization. At point i, tissue A has recovered more than tissue B. Since the magnetization of both tissues still is inverted tissue B will be more intense. At point ii, tissue A has reached positive magnetization, but the signal from tissue B is still stronger. The signal has the same amplitude for both tissues at point iii. After this point the relationship is reversed and the signal is stronger for tissue A, like in point iv. To achieve maximal contrast between tissue A and B, the signal difference should be as large as possible [6]. However if the signal of one of the two tissues are close to zero, the images will not be of much clinical value. This example is applicable in the case of WM and GM where WM has a shorter T1 than GM.

Disadvantages with the MPRAGE sequence are aliasing artefacts if the field of view (FOV) is too small and a long scan time. The total acquisition time is calculated according to,

$$NSA \cdot N_{PE} \cdot \left(N_{slices} \cdot TR + TI + TD\right), \qquad (1)$$

where N_{PE} is the number of phase encoding steps, N_{slices} is the number of slices and NSA is the number of signal acquisitions used for averaging (typically 1). The scan time is however reduced by the use of parallel imaging.

2.2 Volumetric methods

Volumetric measurements in the framework of this project means measurement of the total brain volume and the volume of WM, GM and CSF fluid respectively. Manual analysis of brain volumes is very time consuming when working with 3D images. There is also a risk for variance of the result depending on the observer. In this project locally developed software called Brain Map Statistics (BMAP) has been used for brain tissue segmentation. Brain Map Statistics is a fully automated method for segmentation and tissue classification.

Tissue type segmentation can be considered as an analysis of the image histogram. The image histogram show peak values representing the average signal of different types of tissue. Since the true segmentation is not known, i.e. the separation between different types of tissue in the image histogram, gauss functions can be used to estimate the volume of each tissue type.

The peaks are separated by variations within different tissue classes. However, image noise, intensity inhomogeneities caused by bias field (inhomogeneities of the RF field) and partial volume effects also contribute to the appearance of the histogram. When studying a histogram based on voxel intensity alone these factors also affect the result. Different segmentation and classification models have been developed that takes information of neighbouring voxels into account to decrease the effect of such factors. When one voxel contains two or more different types of tissue the fine structures can not be resolved. The signal from a mixed voxel represents the weighted sum of the signals from each tissue type in the voxel. This is called partial volume effect [5]. Ideally an automated segmentation algorithm should be able to model a mixture of tissues in each voxel instead of a single tissue type in each voxel. An automated model should also be able to generate objective and reproducible results.

Two examples of methods developed for automated segmentation of MR brain images are presented for comparison with BMAP. FMRIB software library (FSL) provides tools for automated segmentation of brain tissue. FSL is freely available for academic use. Statistical Parametric Mapping (SPM) is another alternative for this purpose. SPM is a software package for analysis of brain imaging data. Expectation-Maximization Segmentation is a SPM extension for automated classification of brain tissue in MR images.

2.2.1 Brain Map Statistics

Before tissue specific segmentation is performed with BMAP the brain image is registered to a reference brain. The registration tool corrects each voxel in six different directions; three degrees of rotation and three degrees of translation. The scale of each voxel is kept unchanged to prevent the registration process from altering the result of the volumetric measurement. The difference of the position of each voxel between the reference brain and registered brain is added to a cost function. This cost function is minimized through an iterative process until an indicated degree of accuracy is reached [7]. Variations between different brains due to geometry are removed in the registration process.

Non-brain tissue is roughly cut away by applying a brain template adapted to the same reference brain which is used for the registration. The upper intensity threshold (UT) is found by fitting the down slope of the WM region in the image histogram and extrapolate the fit to the x-axis. The point where this line crosses zero is used to cut off high intensities. This is performed to avoid extreme intensities, arising for example from arteries, to affect the brain tissue segmentation. A lower intensity threshold (LT) is set to 5% of UT to avoid non-brain tissue with low signal, for example bone, to be included in the segmentation (figure 5) [7].

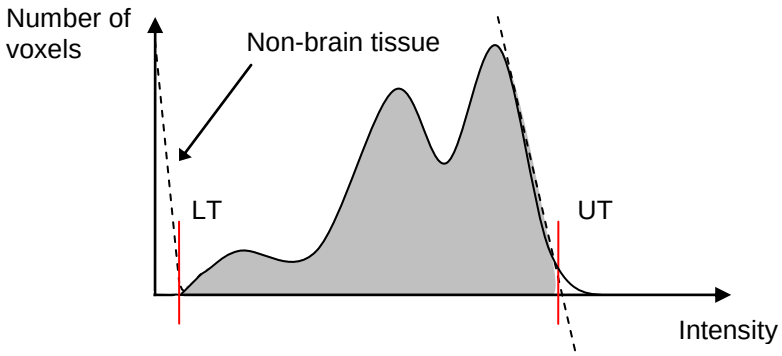

Figure 5. The red line marks where the upper and lower intensity thresholds.

The image is corrected for intensity inhomogeneities caused by signal sensitivity of the head coil and B_1 inhomogeneities. This B_1 inhomogeneity is an effect of increasing field strength and therefore increasing Larmor frequency resulting in shorter wavelengths. The body size becomes significant with respect to the wavelength of the radiation transmitted due to a dielectric resonance effect [8].

The segmentation follows some different steps each given specific criteria. The first step called *grow-mr* (G_1) expands from the centre of the brain template, searching for voxels with intensities in a specific interval. Which voxels are added is determined by the degree of connection to other voxels in the same intensity interval. A larger connection surface corresponds to a higher connection criterion as shown in figure 6 [7]. When the connection criterion is 1 at least one corner between two voxels must be connected. A connection criterion of 2 means that two corners must be connected, either through a co-joining edge between two voxels, or a single corner connection between 3 voxels. The maximum connection criterion possible is 56 which would correspond to a voxel surrounded by 26 other voxels in the same intensity interval.

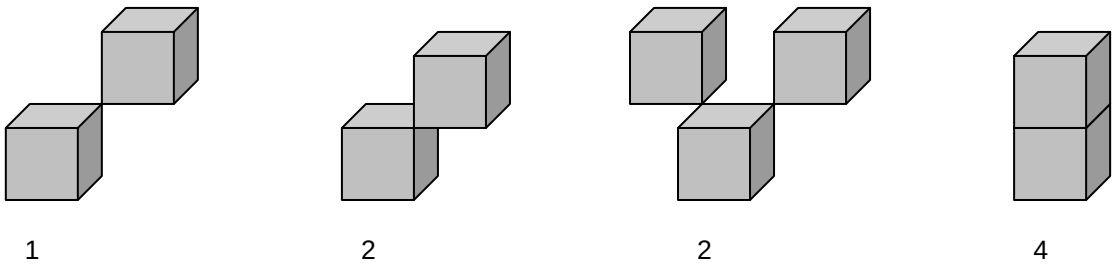

Figure 6. The connection criterion specifies the required degree of connection between a voxel and its neighbouring voxels.

The first G_1 step segments white matter, the intensity criterion is set to find all voxels with intensity between 70-100% of the total intensity range. Here the connection criterion is set to 2. Practically this means that each voxel with intensity $\geq$ 70% of maximum intensity that connects to at least two voxels in the same intensity range by corner, or one voxel by co-joining edge, is added to the growing region. Each G_1 step is looped, usually 200 times. Five different intensity intervals and connection criterions are used to categorize all voxels with white- and grey matter. As the intensity interval is lowered the connection criterion is increased to prevent non-brain tissue from being added to the segmentation. After G_1 the

original MR image is restored followed by the next step, *grow-down* (G_2). The intensity limit in G_2 is decreased to add CSF. When grow down is completed *fill-map* counts all missing voxels in the segmented brain as CSF. After fill map is completed the edges of the segmented brain is smoothed with a convolution matrix. Finally the valleys from the folding of the brain is filled with CSF during the last step, grow erode. Grow erode adds layers of voxels on top of the segmentation, and then removes them again, keeping voxels added in the valleys of the brain. All of these six steps can be altered in a data file called mask file.

There are two different methods of tissue classification available in BMAP; crisp clustering and fuzzy clustering, both illustrated in figure 7. In Crisp clustering all voxels are treated binary which means they are classified as WM, GM or CSF completely. The peak values represent the average signal of each tissue type. All voxels are classed according to which peak they are located closest to. One problem with crisp clustering is that the partial volume effect is not taken into account, each voxel is estimated to consist of just one type of tissue [7].

Fuzzy clustering uses gauss approximations to estimate the volume of WM and GM, CSF is calculated by subtracting WM and GM from the total histogram. One disadvantage with fuzzy clustering is that the overlapping areas between two gauss curves represent voxels with unknown proportions of each tissue type. The overlapping area can be used as an indication of how successful the segmentation is. Small overlapping areas (A and B in figure 7) mean that the different tissue types are more separated in the image histogram. When fuzzy clustering is used partial volume effects are taken into account.

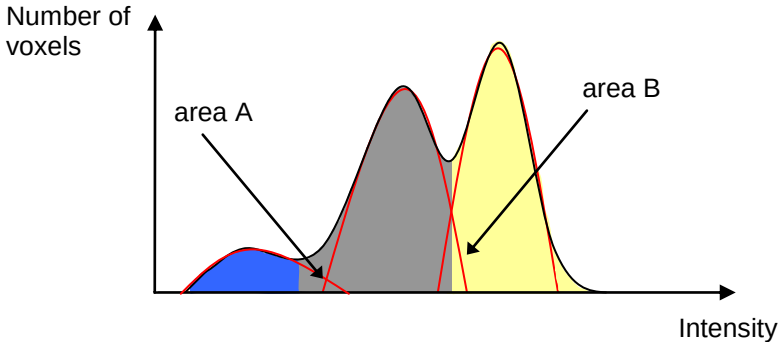

Figure 7. Crisp clustering results in straight borders between the peak values of different tissue types. From left the histogram shows the peaks for CSF, GM and WM. In fuzzy clustering the area under each gauss approximation (red curves) is used to estimate the volume of each tissue type. The distribution of CSF, GM and WM in this figure does not represent the distribution of a real brain.

2.2.2 FSL

For tissue type segmentation tools to perform well, non-brain tissue has to be segmented away from the brain tissue. One tool that can be used for this purpose is Brain Extraction Tool (BET). BET uses a deformable surface model with a tessellated mesh of triangles which is fitted to the surface of the brain. The surface of the mesh is matched with the physical surface of the brain. Physically based constraints are imposed on the surface and information from a large region around each point of interest is used for the matching. The mesh is also smoothed to match the natural smoothness of the brain. The fitting is an iterative process which is repeated with higher smoothness constraints until an optimal solution is found [9]. An example of the resulting mesh is shown in figure 8.

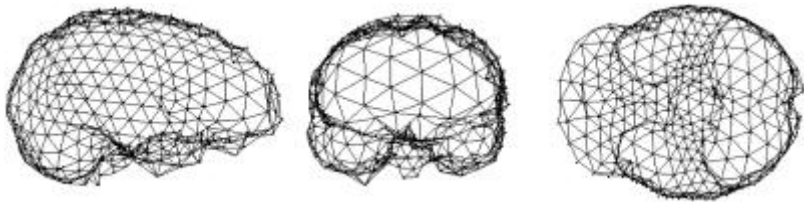

Figure 8. Mesh of triangles fitted to the brain surface (Smith et al. 2002**)**.

At first the image intensity histogram is used to remove small numbers of voxels with intensity values that considerably diverge from the rest of the image. This is carried out by removing the low tails of the histogram. The intensity minimum and maximum are taken as the intensity which lies below 2% and above 98% of the cumulative histogram. High intensity voxels arising from arteries for example are removed this way. Another threshold intensity is chosen to differentiate background and bone from brain matter. This threshold, which is set to 10% of the range between the minimum and maximum intensity, is also used to estimate the centre of gravity (COG) of the brain. A rough estimation of the brain volume is made by counting all voxels with intensity greater than the intensity of the background. The first model of the brain is a sphere of tessellated triangles originating from COG. The radius of the sphere is calculated from the total volume of the voxels with intensity greater than the background. By an iterative process each triangle is subdivided into four smaller triangles and the surface of the sphere is expanded to match the surface of the brain [9].

When the brain/non-brain segmentation is complete, tissue type segmentation can be performed. One common method of tissue type segmentation is analysis of the image histogram based on voxel intensity, used by for example by FMRIB´s Automated Segmentation Tool (FAST). Different tissue classes appear as separate peaks in the image histogram. The peaks are separated by variation within different tissue classes. Other factors like image noise, motion artefacts, partial volume effects and bias field also affect the appearance of the histogram. Gauss functions are used to classify different tissue types. An accurate estimation of the bias field requires knowledge of the segmentation. A perfect segmentation in turn requires that the bias field is known and corrected. These two problems need to be solved together by iterating the estimations until a satisfactory solution is found [10].

To reduce the effect of noise on the segmentation, information from neighbouring voxels is also taken into account. Using Markov random field theory (MRF), the spatial information in an image is encoded through contextual constraints of neighbouring voxels. Neighbouring voxels are by these constraints expected to have the same class labels or similar intensities. Voxels are labelled according to probability values determined from the intensity distribution of the image. With the intensity of each voxel known, the distributions of tissue class labels are assumed through a statistical approach. The statistical approach is solved following certain criterions like maximum likelihood (ML), and Maximum a posteriori (MAP). An expectation-maximization (EM) algorithm is used to solve the ML estimation and determine the model parameters [11].

FAST is able to model the partial volume effect at each voxel using MRF. The intensity of each voxel is compared with the means and variances of neighbouring voxels when the partial volume effect is estimated [10].

To sum up, the segmentation algorithm starts with an estimation of the tissue parameters and tissue classification. The tissue parameters and class labels are then updated iteratively through the EM algorithm. During the iterations tissue class labels and parameters are estimated by MRF and statistical criterions like ML and MAP [11]. The result is a segmentation of brain tissues which is less sensitive to noise, partial volume effects and intensity inhomogeneities than histogram analysis based on voxel intensity alone.

For automated analysis methods like tissue segmentation for volumetric measurements, image registration is needed to make the result reproducible. This reduces the effect of geometric differences between different images. Intensity based registration quantifies the alignment of two images. A cost function is returned after registration parameters like translation and rotation has been matched between the images. One method of optimizing the registration is to start with a poor resolution, when the cost function is returned the registration process is started again with a higher resolution and so forth. One tool for this type of image registration is FMRIB's Linear Image Registration Tool (FLIRT) [10].

Quantitative measurements of the brain size can be used for example to measure atrophy rate of the brain. One FSL tool for measurement of temporal brain change is Structural Image Evaluation using Normalization of Atrophy (SIENA). SIENA uses two MR images taken at two different occasions and returns a change image and an estimate of the percentage brain volume change [12, 13]. SIENA is fully automated, and starts with using BET for brain-non-brain tissue segmentation. Since the images are taken at two different occasions with different geometries, FLIRT is used for registration of the images. Brain surface points are finally found with FAST and the mean perpendicular edge motion across the brain can be converted into a percentage brain volume change. Another FSL tool called SIENAX is used to measure atrophy state by normalizing the brain size for head size [10]. For a complete volumetric measurement all three tools described above; BET, FLIRT and FAST needs to be used. When more than one image is studied image registration to a reference brain is carried out for repeatability of the segmentation. After the registration, brain/non-brain segmentation is implemented to achieve successful brain tissue segmentation.

2.2.3 SPM

The model SPM uses for tissue segmentation is also based on Markov random field theory. The MRF is used both to discriminate between brain and non-brain tissues, and various tissue classes within the brain. The segmentation process can be described as an estimation problem where the segmentation has to be estimated from the observed intensities. A probability density function is parameterized through a random process. A set of parameters is used to model the actual segmentation from the probability density function. Another probability density function is used to describe the observed intensities with a second set of parameters. An estimation of the segmentation can be performed when these model parameters are known. Much like the FAST algorithm in previous section, the SPM model uses an EM algorithm to estimate the maximum likelihood parameters by iterative estimations of the segmentation data. It starts with classification of the voxels, followed by an estimation of the normal distributions and estimation of the intensity inhomogeneities caused by bias field [14]. Segmentations based on the intensity of the voxels alone are limited in the ability of distinguishing between brain matter and non-brain matter. The intensities of different types of tissue surrounding the brain can be close the intensities of WM, GM and CSF. MRF theory is used to introduce constraints about neighbouring voxels to distinguish between brain matter and non-brain matter. Each voxel is given a probability value based on its neighbours used to

determine which tissue type it belongs to. A first ordered neighbourhood system is used, which means that the six nearest voxels are considered [14].

The algorithm used for segmentation performs classification of the voxels, estimates the distribution parameters, the bias field parameters and the MRF parameters. These steps are iterated, starting with classification of all voxels. A digital brain atlas with probability maps for the location of WM, GM and CSF is used for this classification. The brain atlas also helps decreasing the effect of intensity inhomogeneities across the image [14].

Before the segmentation all MR images are co-registered using a method based on maximization of mutual information. It is a voxel similarity based registration method optimizing the similarity of all geometrically corresponding voxel pairs. For intermodal image registration a multi-resolution optimization strategy is used. The mutual information criterion states that the mutual information of the voxel-pairs intensity values is maximal if the images are geometrically aligned. The mutual information matching criterion provides a completely automated registration of MR brain images [15].

The digital brain atlas used for tissue classification is spatially normalized to the study image with the same registration program. When the segmentation starts, voxels where the atlas shows no probability for WM, GM or CSF are removed. The segmentation is carried out iteratively until the relative change of the estimation of log likelihood between two iterations become smaller than 0.0001. This typically occurs after 25 iterations [14].

2.2.4 Comparison between segmentation tools

Brain Map Statistics, FSL and SPM all use similar methods for tissue type segmentation. For volumetric measurements an image registration is needed to get a repeatable result independent of method used for segmentation. FSL has a separate tool for brain/non-brain segmentation whereas this function is embedded in SPM and BMAP. One advantage with BMAP is that the degree of connection to neighbouring voxels can be varied. SPM uses a first ordered neighbourhood system which means that the six nearest neighbours are used. All parameters in BMAP can easily be changed in order to optimize the segmentation for a specific MR sequence. Each step of the segmentation process is visualized, which makes it easier to find an error if something does not work properly. Brain Map Statistics has four different intensity inhomogeneity correction algorithms to choose from.

2.3 The optimisation procedure

The segmentation result depends on many factors, for instance image noise, spatial intensity variations caused by signal sensitivity of the head coil, B_1 inhomogeneities, partial volume effects and variations within different tissue classes. B_0 inhomogeneities can be reduced by using shimming before each examination. The effect of B_1 inhomogeneities and coil sensitivity can be reduced by the use of a suitable intensity correction algorithm. The image SNR is increased by using a 3T MRI unit which gives more signal than a 1.5 T. Parallel imaging is also used to increase SNR, or decrease the acquisition time. The partial volume effect can be reduced by using a small voxel size, at the cost of a decreased SNR. The partial volume effect can also be estimated using fuzzy clustering as mentioned above.

The highest intensity from brain tissue is generated by WM, followed by GM and CSF. The image histogram has three intensity peaks from the right (figure 9). Each peak value represents the mean signal intensity for WM, GM and CSF respectively. The WM- and GM peak values are used for the gauss approximations in fuzzy clustering to estimate the volume

of each tissue type. The peak values can also be used to calculate the tissue contrast between WM-GM and GM-CSF according to,

$$C_r = \frac{(S_1 - S_2)}{(S_1 + S_2)}. \quad (2)$$

The values S_1 and S_2 represent the peak values of WM and GM for WM-GM contrast or GM and CSF for GM-CSF contrast.

Parameters that can be changed in the MPRAGE sequence to vary the relative tissue contrast relationship are the inversion time (TI) and flip angle (FA). The nature of these contrast relationships is described in section 2.1. By varying both TI and FA and using all combinations of the two parameters the optimal contrast relationship between WM, GM and CSF can be found. In order to investigate which set of sequence parameters is optimal the image histogram is used with fuzzy clustering. Firstly the overlapping areas between WM-GM and GM-CSF are examined. The overlapping area should be as small as possible when the tissues are well separated and the segmentation is successful. The overlapping area is calculated in percent of the total volume. The total volume in turn is calculated as the sum of volumes from the gauss approximations of WM, GM and the CSF volume. Secondly, peak distances between the different tissue types are compared, a long peak distance between two tissue types also means that the tissues are well separated.

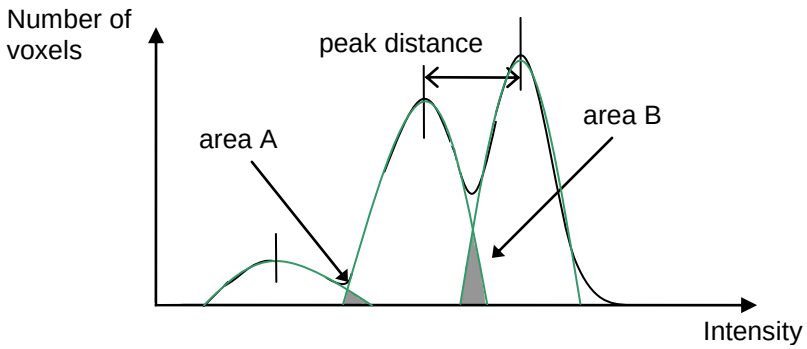

Figure 9. Area A shows overlapping area of the approximated gauss functions from CSF/GM, area B shows the corresponding area for GM/WM. Peak distance is shown between GM-WM.

The contrast ratio between different tissue types is also compared. Since the contrast ratio is calculated from the peak values it is related to the peak distance. The sequence which gives the best total result for all of these parameters when WM, GM and CSF are considered is sought.

2.4 Parallel imaging

3D MRI sequences with a long repetition time, and in the case of MPRAGE a delay time, are often quite time consuming. Parallel imaging can be used to reduce the imaging speed. In parallel imaging many parallel independent receiver coils are used (phased array coils) to collect the signal. The use of phased array coils results in an increase of SNR. This way the number of phase encoding steps can be reduced with maintained resolution and without a detrimental decrease of SNR. The reduction of phase encoding steps results in a reduction of the total scan time [16].

2.4.1 Acquisition technique and image reconstruction

A coil that receives signal from any given voxel also receives noise that is proportional to the integrated sensitivity of the coil over the whole sample. This means that the SNR performance at a specific voxel is worse for a large coil than a small coil. To use this better SNR performance and still be able to receive signal from larger areas than a small coil can receive alone, multiple small elements are used in an array coil. Each specific element in an array coil needs an individual receiver system [17].

In order to reconstruct images from the under sampled k-space data, an image reconstruction algorithm is needed. Basically there are two different kinds of reconstruction methods used in parallel imaging. One is working in the image domain. When the number of phase encoding steps is decreased aliasing artefacts will be introduced in the images. By combining images from several different coil elements these artefacts can be removed. Both the coil reference data and the sub-sampled target data are operated in the image domain. This algorithm is called SENSE (SENSitivity Encoding) [16].

The second type of reconstruction algorithm is working in the frequency domain. This type of reconstruction algorithm is used in this project and is called GRAPPA (GeneRalized Auto calibrating Partially Parallel Acquisition) [18]. GRAPPA is a fast reconstruction method working entirely in k-space. Each coil produces separate sets of k-space data. In the centre of k-space multiple reference lines are acquired which are used to reconstruct the missing k-space data from each coil. One image is reconstructed for each coil element. The images are combined by a sum of squares algorithm to obtain the final image. Since more than one reference point is used to reconstruct each missing point of k-space data the accuracy of each reconstructed point is good. This reduces the dependence of the geometry of the coil array used and hence reduces the g-factor which is described in the following section [17].

2.4.2 Benefits and drawbacks of parallel imaging

With parallel imaging a higher resolution or a decrease in scan time can be achieved. A shorter scan time reduces the risk of motion artefacts since the time the patient has to lie still is decreased. The time reduction with parallel imaging comes with a cost of decreased SNR and a risk of artefacts. The change of SNR depends on two factors; the reduction is proportional to the square root of the time reduction factor (r), and the geometry factor (g-factor). The g-factor, which depends on the geometry of the coil array, measures the level of noise amplification that results from the reconstruction. The value of the g-factor depends on the ability of the coils to distinguish the signal contribution from different locations. It is therefore dependent on the number and configuration of the coils. The SNR relationship in one voxel as a function of time reduction and the g-factor can be described by;

$$SNR_{voxel}^{red} = \frac{SNR_{voxel}^{full}}{g_{voxel}\sqrt{r}}. \qquad (3)$$

It has been shown by Lindholm et al. that parallel imaging can be used without detrimental effect to brain tissue segmentation and volumetric measurement at a 1.5 T MRI unit [19]. It has also been shown by Masanobu et al. that the results of Voxel-based Specific Regional Analysis System for Alzheimer's Disease (VSRAD) for images acquired with and without the SENSE method are nearly equal [20].

3 MATERIALS AND METHODS

A prestudy with MRI test objects was conducted in order to make a first approximation of the range of flip angle and inversion time that should be tested in the volunteer study. The test objects consist of tubes with agarose gel simulating WM and GM.

In a second prestudy the mask file described in section 2.2.1 was optimized. Two brain images were segmented using six different mask files with different criteria of intensity constraints during the growing steps of the segmentation processes. When the most suitable mask file had been chosen, a third prestudy was performed using 2 volunteers to decide the final scan protocol for the main volunteer study. The main study included 9 volunteers aged 22-41 years (5 men and 4 women). The volunteers were scanned according to the resulting scan protocol from prestudy 3. The results from the volunteer study were used to choose which set of parameters that should be used for an optimal segmentation result. Finally one volunteer was scanned several times with the optimal contrast parameters to evaluate the repeatability of the brain tissue segmentation.

3.1 Shimming and intensity correction

Before the volunteer study, the effect of magnetic field inhomogeneities (B_0) was examined with a spherical oil phantom and one volunteer using the 32 channel head coil. Both the phantom and the volunteer were scanned with automatic shimming and with manual shimming of the main magnetic field. A flip angle of 9º and inversion time of 800 ms was used. The intensity profiles and segmentation results from the images were compared in order to decide if manual shimming was necessary or not in the volunteer study. Distortions of brain images can be hard to observe because of the small anatomical structures. This is why a phantom also was used, to spot major distortions. The effect of spatial intensity variations in the images caused by signal sensitivity of the head coils and B_1 inhomogeneities was also examined. This was done by studying the image intensity profiles before and after intensity correction was carried out on a segmented brain image acquired with the 32 channel head coil. All intensity corrections have been performed in BMAP.

3.2 Prestudy 1 – MRI test objects

The test objects used in this study consists of agarose gel doped with Gadolinium enclosed in tubes. A set of 18 tubes with varying T1- and T2 relaxation times due to various compositions of gel and Gd were available. The manufacturer of the tubes (Diagnostic Sonar LTD, Livingston, Scotland) has listed T1 and T2 at room temperature (296 K) for 7 different field strengths (0.02; 0.15; 0.28; 0.5; 1.0; 1.5 and 2.0 T). The relaxation time was plotted as a function of field strength B_0 in Excel, and logarithmic curve fitting was used to find T1 and T2 for a field strength of 3 T. Two tubes with relaxation times in a range close to that of WM and GM at 3T were used in the study. The actual relaxation times are shown in table 1.

Table 1. Relaxation times of test objects at 3T and reference values for WM and GM. The deviation of the reference values derives from different ROI locations and sex of the subjects [21].

	WM test tube	WM literature	GM test tube	GM literature
T1 [ms]	555	832 ± 10	1110	1331 ± 13
T2 [ms]	92.8	79.6 ± 0.6	131.5	110 ± 2

The test tubes were attached to a larger oil phantom to load the head coils (see figure 10). The two tubes were scanned with varying FA; 8, 9, 10, 11 and 12°. For each value of FA, TI was set to 711, 800, 900, 1000, 1100 and 1200 ms. 711 ms was the shortest TI possible without increasing the bandwidth (BW) which would result in more recorded noise and hence

decreased SNR. A small cubic voxel size of 1 mm^3 was used. The other parameters were set to 190 kHz BW, 176 slices per slab, repetition time (TR, of the whole sequence) 1900 ms, echo time (TE) 2.52 ms and matrix size 256 · 256.

Figure 10. The test objects used in this study. The two dots at the top are the WM gel (left) and GM gel (right). The dot at the left side is a marker for orientation and the black sphere is the oil phantom.

Two sets of images were obtained, one from the 12 channel coil, and one from the 32 channel coil. The signal from the tubes was averaged from a cross sectional area over 3 different slices of the test objects. The region of interest (ROI) covered 70% of the cross sectional area of the test objects. The contrast ratio (C_r) between WM and GM was calculated according to equation 2 in section 2.3. The calculated signal from the test tube representing WM was denoted S_1 and the calculated signal from the test tube representing GM was denoted S_2.

3.3 Prestudy 2 – Optimization of the mask file

The parameter values in the mask file i.e. intensity intervals, connection criteria and the number of loops had already been optimized when the mask file was created. The lower intensity limit needed some fine tuning in order to get rid of as much non-brain tissue as possible without discriminating actual brain tissue. Six different intensity intervals were tested (for details, see appendix A). This was performed for two sequences, one with the parameters (FA and TI) set to obtain high brain tissue contrast, and one sequence with low brain tissue contrast, both shown in table 2.

Table 2. Sequence contrast parameters.

	Flip angle º	Inversion time [ms]
High brain tissue contrast	9	800
Low brain tissue contrast	11	1000

One volunteer was scanned with both sequences, using both the 12 channel- and 32 channel head coils. In essence, four different scans were performed, two for each head coil. The image data of each scan was segmented with six mask files using different lower intensity limits.

Firstly a visual inspection of the masking result was performed to make sure that the borders of the brain were treated correctly. Secondly, six different parameters were evaluated; peak distance WM-GM and GM-CSF, image contrast WM-GM and GM-CSF, overlapping area WM/GM and GM/CSF. The peak distance can easily be calculated by subtraction of the peak values in the histogram resulting from the segmentation. The tissue contrast is calculated according to equation 2 in section 2.3. The overlapping areas from the Gauss approximations are given by BMAP.

Each parameter once quantified was normalized to the best result. The sum of the value from all six parameters represents a total grade for each mask file. An optimal mask file would have the grade 6 (100%) if it performed best in all six parameters evaluated. The total volume and the proportion of WM and GM to the total volume (Brain Parenchymal Fraction, BPF) were also evaluated. If the total volume is discrepant from the average volume it may be due

to a loss of brain matter or that non-brain tissue has been included during the segmentation. This is often verified by visual inspection of the slices of the segmented brain.

3.4 Prestudy 3 – Selection of scan protocol

The third prestudy involved two volunteers. The volunteers were scanned with both head coils and the parameters in table 3.

Table 3. Scan protocol for prestudy 3.

Parameter	Volunteer 1	Volunteer 2
FA [deg]	8, 9, 10, 11	8, 9, 10
TI [ms]	700, 800, 900, 1000	800, 900, 1000
TR [ms]	1900	1900
TE [ms]	2.52	2.52
TD [ms]	~ 300	~ 300
Matrix size	256 · 256	256 · 256
Number of slices	176	176
iPAT	2	2
Voxel size [mm^3]	1 · 1 · 1	1 · 1 · 1

TD varies automatically when the other imaging parameters are changed but is close to 300 ms. Artefacts may appear when the FOV is smaller than the area of the object that is scanned. Signal originating from regions outside FOV may be causing wrap-around in the image. The FOV is kept as small as possible in the phase encode direction in order to shorten the scan time, whilst ensuring no harmful wrap-around effects occurs. iPAT is Siemens term for acceleration factor when using parallel imaging. The total scan time is about four minutes per sequence. All series of images were analysed in BMAP with the mask file chosen in prestudy 2. The results were evaluated the same way as in prestudy 2, with respect to peak distance, image contrast and overlapping area. Images acquired with FA = 8, 9 and 10° and TI of 800 and 900 ms were evaluated by an experienced neuro-radiologist in terms of tissue contrast for clinical diagnosis.

3.5 Volunteer study

The volunteer study is subdivided into four different sections, starting with the optimization of contrast parameters performed using 9 volunteers. When the optimized contrast parameters had been found the images were evaluated by a neuro-radiologist. Finally a comparison was made between the two head coils, and the repeatability was tested by scanning one volunteer many times using the same image contrast parameters.

3.5.1 Optimization of contrast parameters

The volunteer study involves 9 healthy volunteers (5 men and 4 women) aged 23-41 years. All test subjects were scanned with the parameters in table 4, using both the 12 and the 32 channel head coils.

Table 4. Scan protocol for the volunteer study.

Parameter	Value
FA [deg]	8, 9
TI [ms]	800, 850, 900, 950
TR [ms]	1900
TE [ms]	2.52
TD [ms]	~ 300
Matrix size	256 · 256
Number of slices	176
iPAT	2
Voxel size [mm^3]	1 · 1 · 1

The results were evaluated the same way as in prestudy 2 and 3 with respect to peak distance WM-GM and GM-CSF, overlapping area between WM/GM and GM/CSF and contrast ratio between WM/GM and GM/CSF. Each of the six parameters was normalized to the highest value resulting in a score ≤ 1. This score of each parameter, for all of the images, was summarized to a total score where the maximum result possible is 6. The images were ranked by this total score where all parameters are taken into account. The result of the grading is presented in percent where a score of 6 corresponds to 100%. A sequence with a score of 100% does not mean that the segmentation result is perfect, just that it is the best sequence tested according to this grading system.

The contrast to noise ratio (CNR) was calculated as a function of sequence and coil for all volunteers. CNR is calculated by dividing the signal difference between two tissues (S_1 and S_2) by the standard deviation of the background signal;

$$CNR = \frac{S_1 - S_2}{SD_{bkg}}. \qquad (4)$$

A region of interest was drawn at the upper right corner of one slice from one brain image. This ROI was copied to five slices equally distributed over the volume. The average standard deviation of the background signal was measured in this way in all images.

3.5.2 Evaluation by neuro-radiologist

The resulting images were evaluated by a consultant neuro-radiologist. The neuro-radiologist was asked to grade the images on a scale from 1 to 5 in terms of tissue contrast for clinical diagnosis. Grade 1 means that the images are not useful on the basis of these criteria. Grade 3 means that the images are approved, and 5 that the image quality is excellent. Grades 2 and 4 are steps between these extremes. From the repeatability study 6 images were evaluated, 3 from each coil. Eight images from the volunteer study were evaluated. The sequence parameters of these images were FA = 8° and TI = 800 and 850 ms, both coils and two subjects were compared. Information about coil and sequence parameters was not known to the neuro-radiologist.

3.5.3 Comparison between the 12- and 32 channel head coils

The acquired data from the optimization study was analyzed for a theoretical comparison between both head coils used. The statistics program Statistica (StatSoft, Scandinavia AB) was used to make a statistical analyze of the image data.

3.5.4 Repeatability study

When the optimal sequence parameters had been determined the repeatability of the segmentation result was examined. This was performed by scanning one volunteer 6 times with each head coil using the optimized contrast parameters. The test subject was instructed to stand up and walk around a few steps between each scan. The images from the repeatability study were also used to measure the standard deviation of the background signal as described above, and make a comparison of the CNR between both head coils.

4 RESULTS

4.1 Shimming and intensity correction

Intensity profiles from the oil phantom used to investigate the differences between manual- and automatic shimming is shown in figure 11.

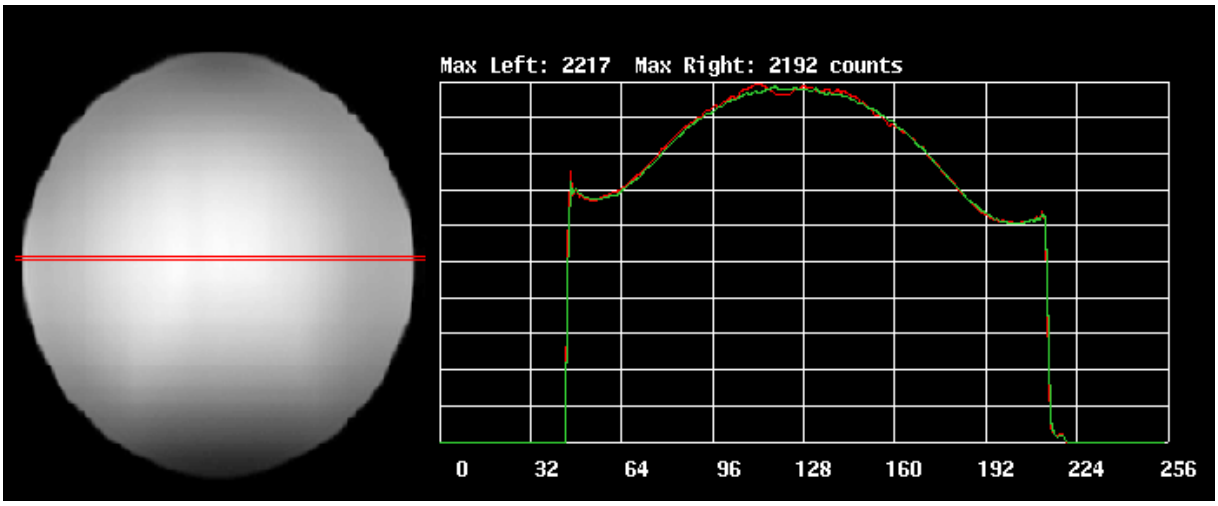

Figure 11. Oil phantom, red profile with automatic shimming and green profile with manual shimming.

There are some inhomogeneities with automatic shimming which is shown at the top of the red intensity profile. The green intensity profile shows the oil phantom with manual shimming.

The segmentation results for brain images with automatic- and manual shimming are shown in table 5.

Table 5. Segmentation results of brain images with automatic shimming, and with manual shimming of the main magnetic field. The deviation of the segmentation result from the image without shimming is shown in the right column.

Parameter	Automatic shimming	Manual shimming	Auto shim./ man. shim. [%]
Total volume [ml]	1597.61	1590.35	1.00
BPF [%]	95.04	95.49	1.00
Peak dist. WM-GM	85	84	1.01
Peak dist. GM-CSF	115	120	0.96
Overlap. WM/GM [%]	11.40	11.14	1.02
Overlap. GM/CSF [%]	2.80	2.89	0.97
Cr(WM-GM)	0.175	0.169	1.03
Cr(GM-CSF)	0.401	0.408	0.98

Intensity profiles of a masked brain with- and without correction for intensity inhomogeneities are shown in figure 12.

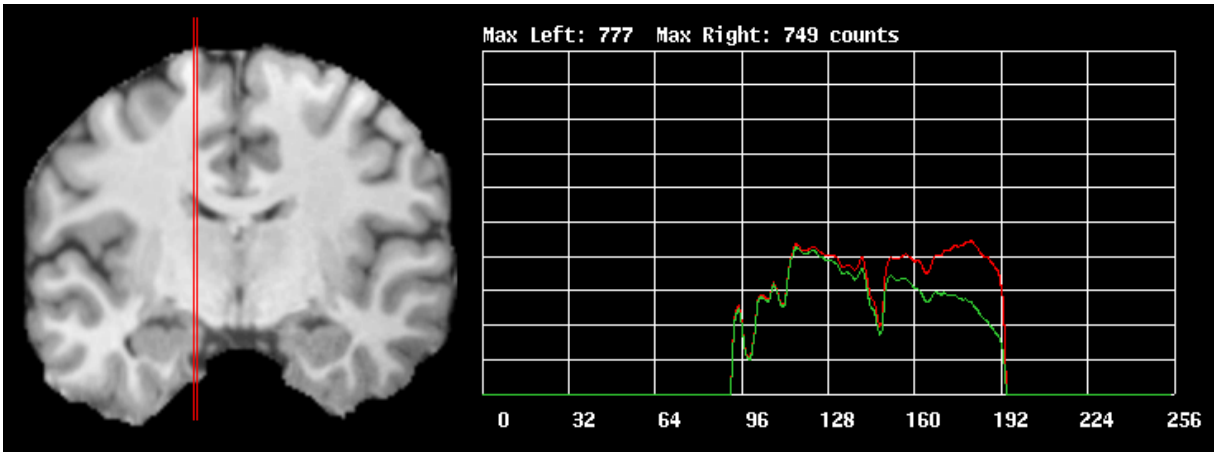

Figure 12. Brain image, red profile with intensity correction and green profile without intensity correction.

The brain images have both been registered to a reference brain. The red intensity profile represents the brain image with intensity correction and the green intensity profile represents the same brain without intensity correction. The green intensity profile from the uncorrected image shows a decreased intensity at the base of the brain.

4.2 Prestudy 1 – MRI test objects

The results of the first study can be seen in figures 13 and 14. The figures show how the contrast ratio between the test objects varies with FA (series) and TI (x-axis). For the 12 channel coil there is a maximum Cr for FA = 10° and TI = 711 ms. The contrast ratio decreases for all TI longer than 711 ms. The largest difference in Cr(WM-GM) as a function of TI was found for FA = 8°, where Cr(TI=1200) was 69% of Cr(TI=700).

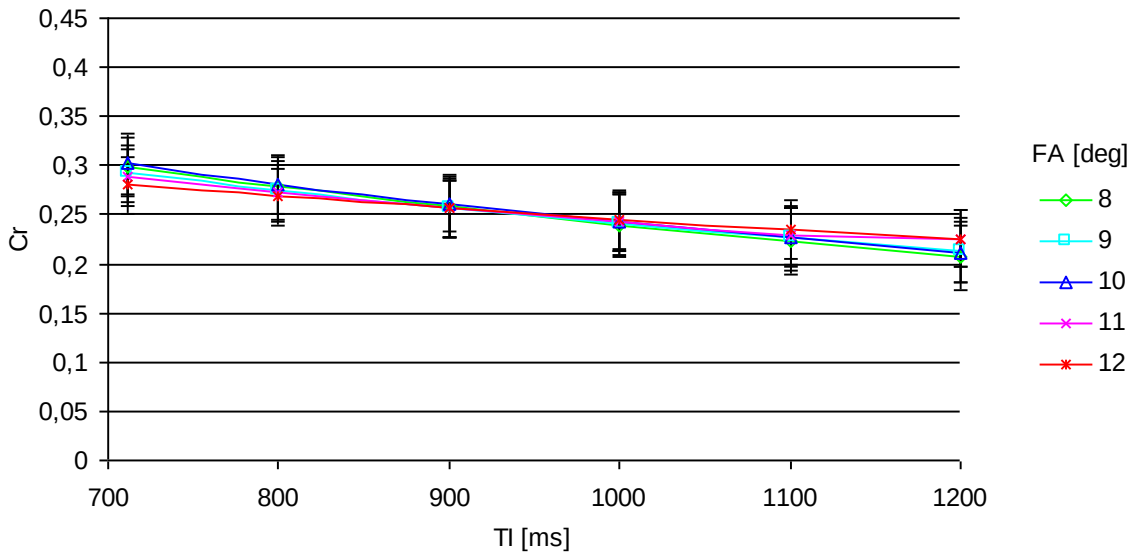

Figure 13. Contrast ratio is shown as a function of TI for different FA. MPRAGE sequence with a 12 channel head coil was used.

For the 32 channel coil the characteristics are similar, but more pronounced. The maximum Cr can be found at FA = 8°, Cr then decreases with increasing TI. The difference between different FA is greater for short TI. The largest difference in Cr(WM-GM) as a function of TI was found for FA = 8 °, where Cr(TI=1200) was only35% of Cr(TI=700).

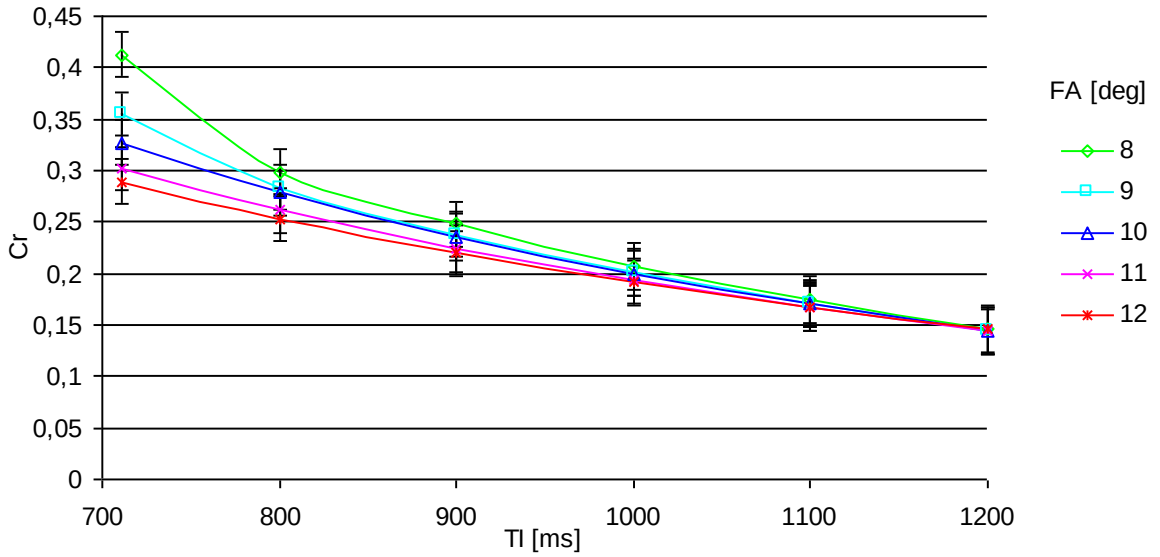

Figure 14. Contrast ratio is shown as a function of TI for different FA. MPRAGE sequence with a 32 channel head coil was used.

4.3 Prestudy 2 – Optimization of the mask file

The visual inspection of how the borders of the brain are treated was quite satisfying for all different mask files, the result can't be used to exclude any mask file. In figure 15 some example slices from a segmented brain image are shown. As can be seen on slices 60 and 70 the masking process is not always perfect, here some non-brain tissue is visible at the right occipital-, parietal- and temporal lobes.

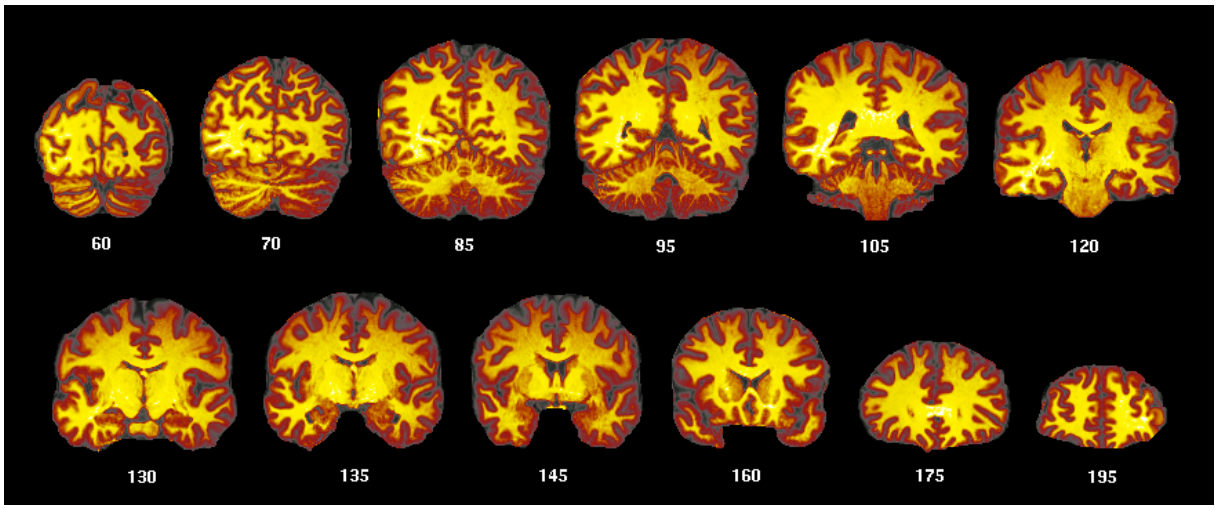

Figure 15. Example slices of the brain after segmentation.

Results from the grading of the mask files as described in section 3 are shown in table 6.

Table 6. Results from grading of the mask files.

Coil/sequence	Mask file no.	Placing	% (of max)
12 high Cr	1	**1**	92.6
	5	**2**	92.5
	2	**3**	90.6
32 high Cr	1	**1**	99.1
	2	**2**	96.1
	4	**3**	96.2
12 low Cr	1	**1**	98.3
	2	**2**	98.2
	6	**3**	98.2
32 low Cr	5	**1**	98.3
	3	**2**	96.6
	2	**3**	96.5
Total 12 & 32	1	**1**	96.6
	3	**2**	95.5
	6	**3**	92.4

The different settings in mask file 1-6 is shown in appendix A. Mask file number 1 reached the highest grade for both sequences with the 12 channel coil, and the high contrast sequence with the 32 channel coil. Altogether mask file 1 got the best result.

The difference in total brain volume and BPF as a function of mask file (x-axis) and sequence/head coil (series) are presented in figures 16 and 17.

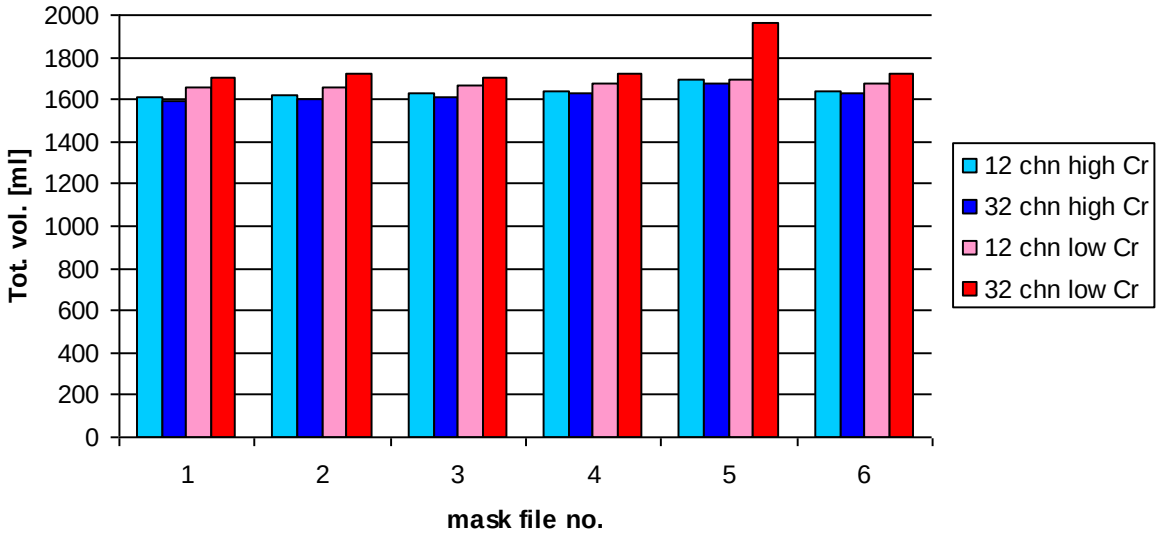

Figure 16. Total volume of WM + GM + CSF for both head coils and sequences as a function of mask file.

The largest difference of the total volume as a function of head coil for the high contrast sequence was found for mask file 5 where vol.(32chn) was 98.4% of vol.(12chn). The smallest difference was found for mask file 1 where vol.(32chn) was 99.3% of vol.(12chn). For the low contrast sequence the largest difference was also found for mask file 5 where vol.(12chn) was 84.0% of vol.(32chn). The smallest difference was found for mask file 3 where vol.(12chn) was 97.2% of vol.(32chn).

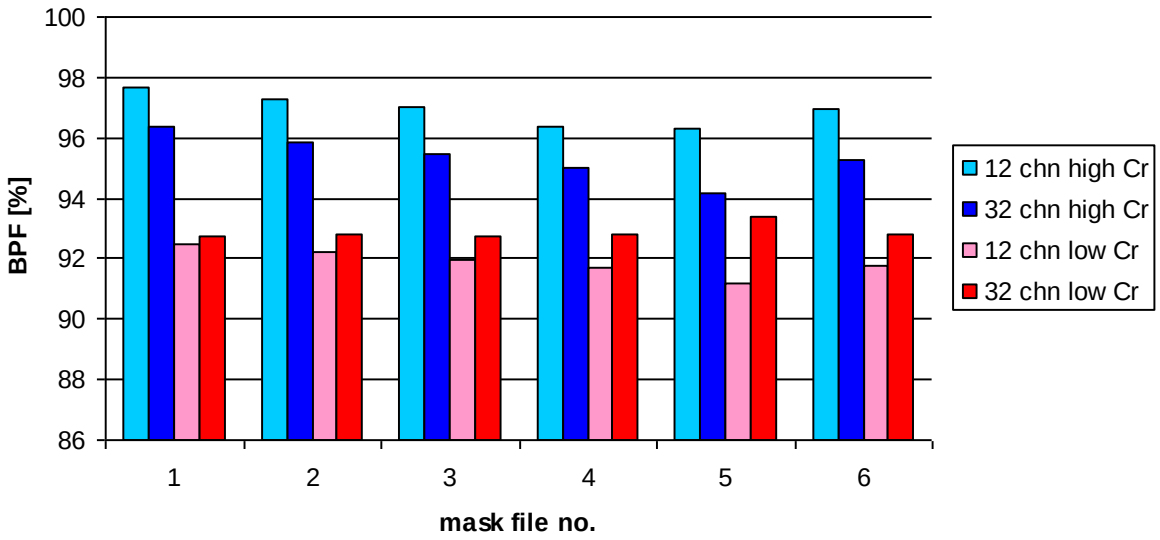

Figure 17. Brain Parenchymal Fraction for both head coils and sequences as a function of mask file.

The largest difference of BPF as a function of head coil for the high contrast sequence was found for mask file 5 where BPF(32chn) was 97.9% of BPF(12chn). The smallest difference was found for mask file 1 where BPF(32chn) was 98.7% of BPF(12chn). For the low contrast sequence the largest difference was also found for mask file 5 where BPF(12chn) was 97.7% of BPF(32chn). The smallest difference was found for mask file 1 where BPF(12chn) was 99.7% of BPF(32chn).

4.4 Prestudy 3 – Selection of scan protocol

Figures 18 and 19 shows the volume of GM, WM, CSF and the total brain volume for volunteer 1. The variation of the total volume as a function of FA for the 12 channel coil, shown in figure 18, is only 5%. However it can be seen that the volume of CSF was zero for FA = 8, 9, 10º and close to zero for FA = 11º when TI is set to 700 ms.

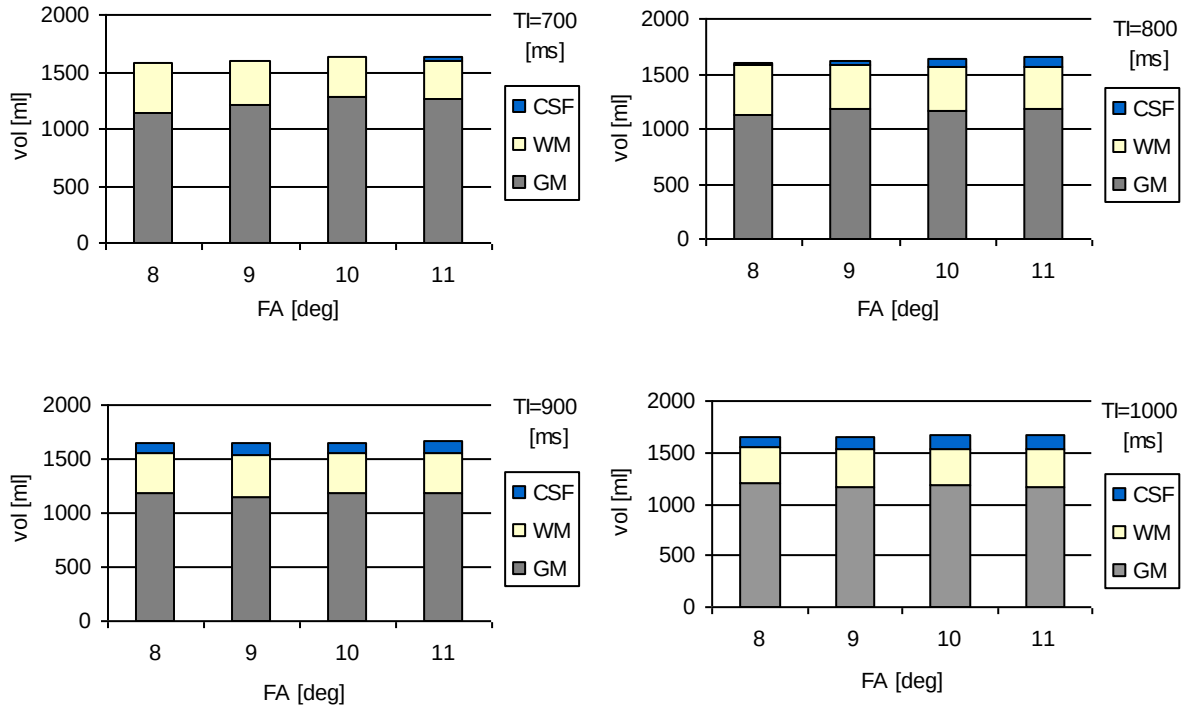

Figure 18. Volumes of GM, WM and CSF as a function of flip angle for the 12 channel head coil. There is one plot for each inversion time.

The variation of the total volume for the 32 channel coil shown in figure 19 is 19%. If all sequences with TI = 1000 ms are removed, the variation of the total volume is reduced to 6%. The 32 channel coil also results in zero or close to zero volume of CSF for TI = 700 ms.

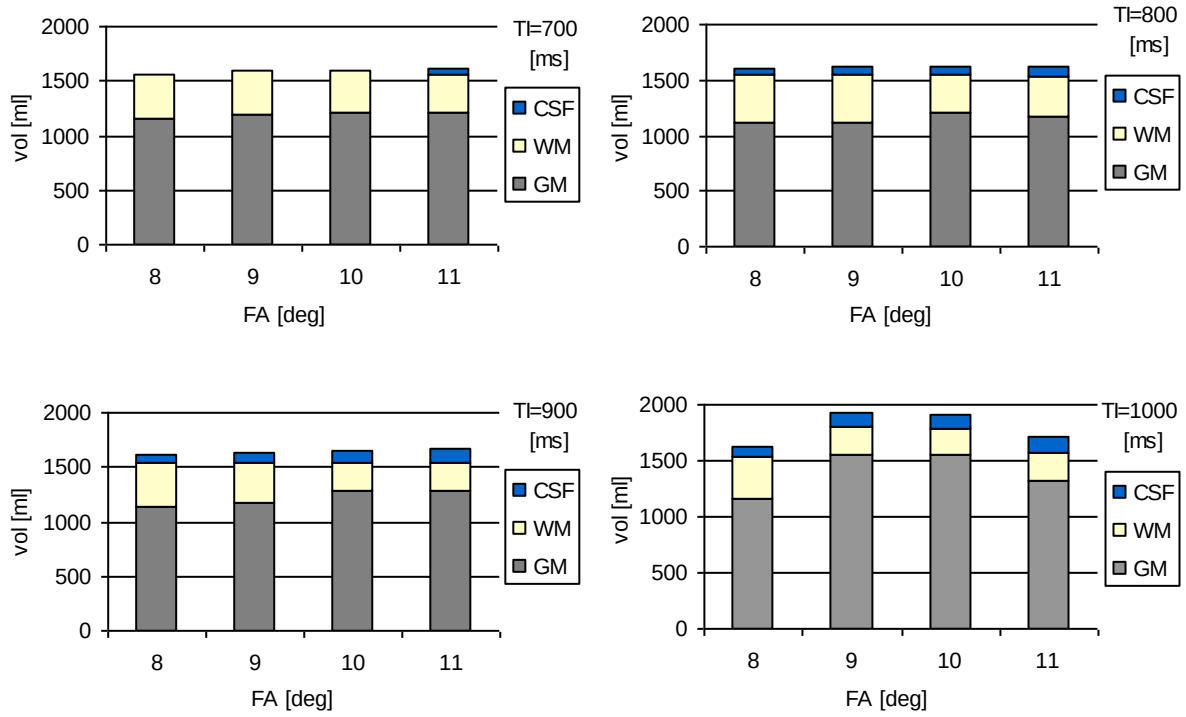

Figure 19. Volumes of GM, WM and CSF as a function of flip angle for the 32 channel head coil. There is one plot for each inversion time.

These results indicate that there is a stabilization of the CSF volume at inversion times longer than 800 ms.

Figure 20 shows the overlapping area as a function of FA (x-axis) and TI (series) for the 12 chanel coil (top) and the 32 channel coil (bottom). The overlapping area between GM and WM becomes smaller for small FA and short TI with both coils. A small overlapping area is desirable. The spread in resulting overlapping areas is less for the 12 channel coil than for the 32 channel coil for a given FA.

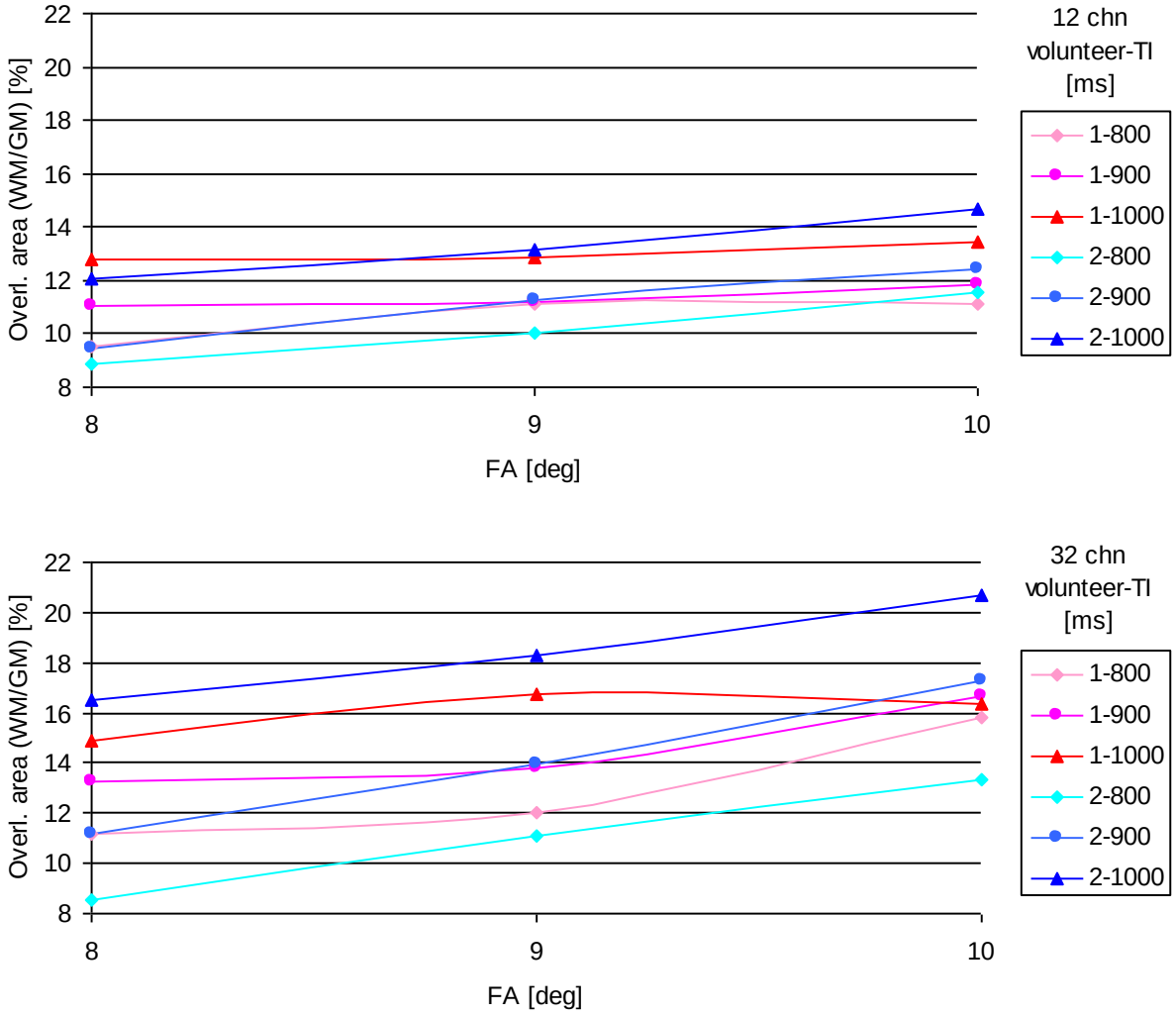

Figure 20. Overlapping area as a function of FA for different TI between GM and WM for volunteer 1 (red tones) and 2 (blue tones) for both the 12 channel coil (top) and 32 channel coil (bottom).

Figure 21 shows the peak distance between GM-WM as a function of FA (x-axis) and TI (series) for the 12 channel coil (top) and 32 channel coil (bottom).. The peak distance increases with decreasing FA and TI. Long peak distance means good contrast between WM and GM and a more correct segmentation. The spread in resulting peak distances is less for the 12 channel coil than for the 32 channel coil for a given FA.

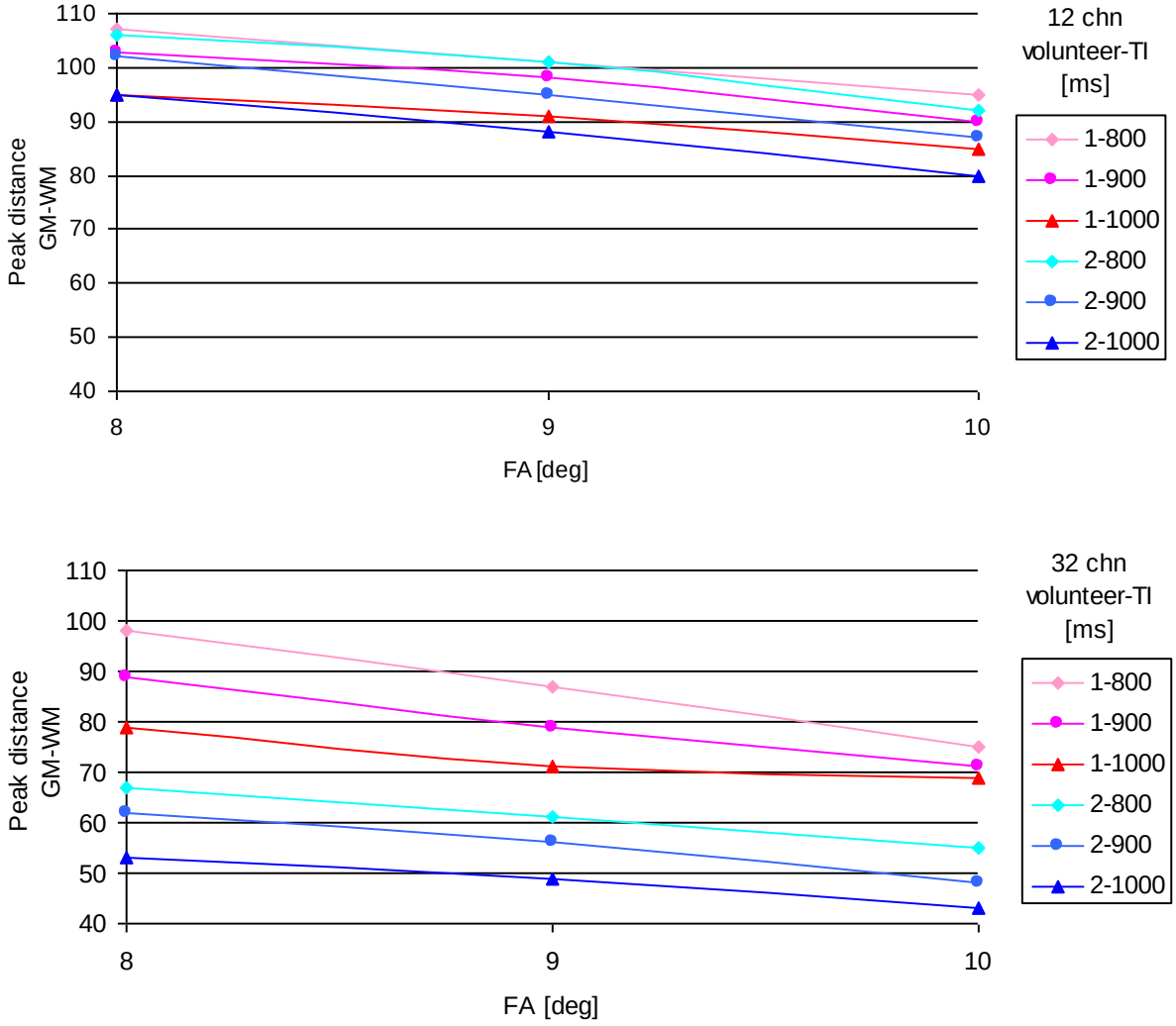

Figure 21. Peak distance as a function of FA for different TI between GM and WM for volunteer 1 (red tones) and 2 (blue tones) for both the 12 channel coil (top) and 32 channel coil (bottom).

Figure 22 shows Cr between WM-GM as a function of FA (x-axis) and TI (series) for the 12 channel coil (top) and the 32 channel coil (bottom). The contrast ratio is higher for smaller FA and shorter TI. Cr is slightly higher for the 12 channel coil than the 32 channel coil.

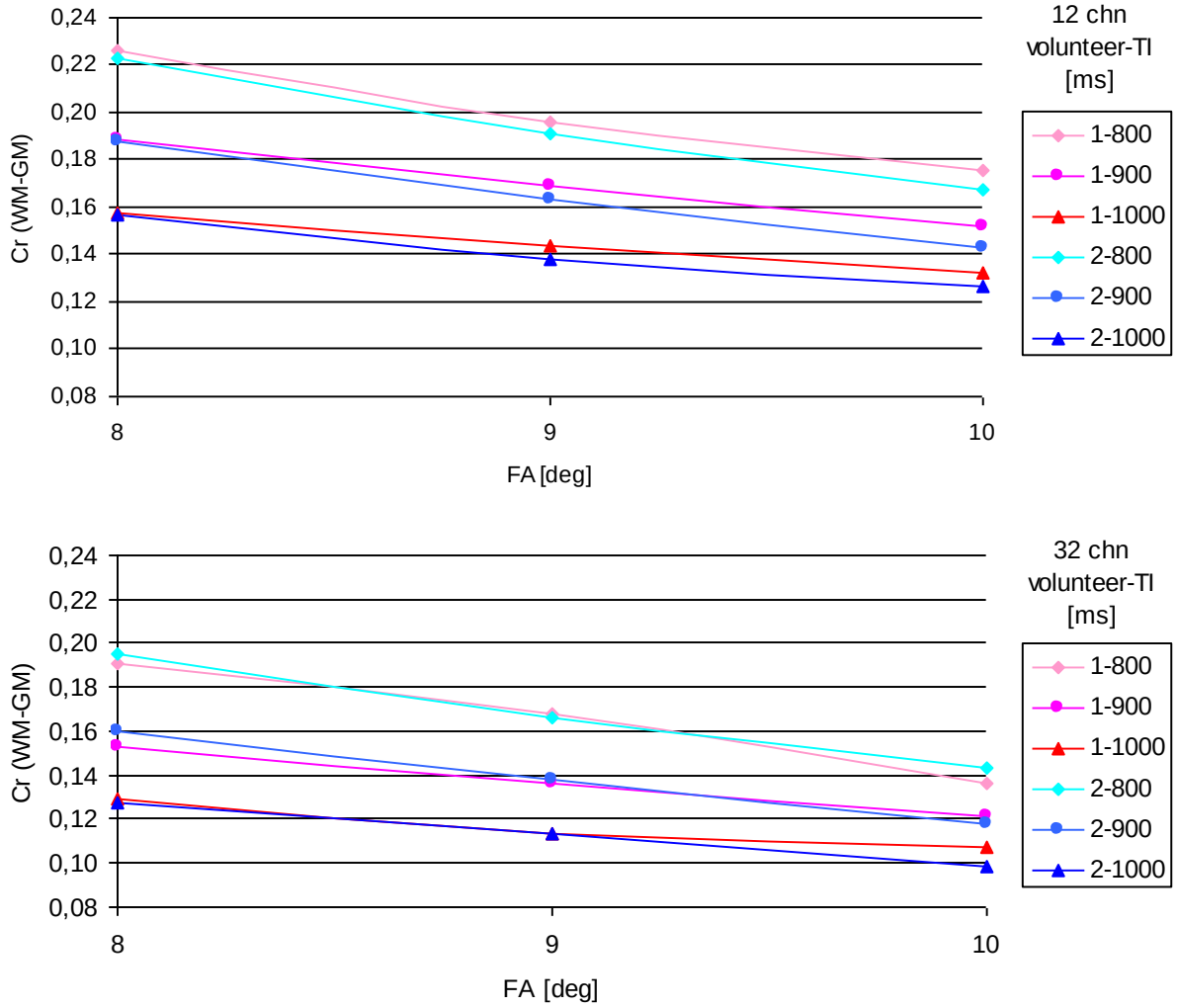

Figure 22. Contrast ratio as a function of FA for different TI between GM and WM for volunteer 1 (red tones) and 2 (blue tones) for both the 12 channel coil (top) and 32 channel coil (bottom).

Results from the grading of the sequences, performed using the same method as described in section 3.3, are shown in table 7. The sequences with FA of 8 or 9º and TI of 800 or 900 ms got the best results.

Table 7. Results from grading of the sequences.

coil	FA	TI	% (of max)
12	8	800	74.0
12	9	900	70.8
12	8	900	67.4
32	8	900	88.8
32	9	900	75.8
32	8	800	75.0

The result of the evaluation of the images by a neuro-radiologist was satisfying. All images acquired with FA = 8, 9 and 10° and TI = 800 and 900 ms was acceptable from a clinical point of view. The neuro-radiologist judged the images from the 32 channel coil as smoother. The possibility of dissolving fine anatomical details was varying between the coils for different contrast parameters. The 32 channel coil was judged to be slightly better at showing anatomical detail for small FA and short TI in the intervals that were evaluated.

4.5 Volunteer study

The contrast parameters used in sequence 1-8 in the following figures (figure 23-32) are shown in table 8. A flip angle of 8° is used in sequence 1-4 and 9° in sequence 5-8. The series in figure 24-32 are divided into two parts to show how the parameters vary with TI for both flip angles.

Table 8. Image contrast parameters for sequence 1-8.

Sequence	FA°	TI [ms]
1	8	800
2	8	850
3	8	900
4	8	950
5	9	800
6	9	850
7	9	900
8	9	950

4.5.1 Optimization of contrast parameters

The result of the grading of the sequences is shown in figure 23 for 12 channel- and 32 channel head coils. All six parameters (peak distance WM-GM and GM-CSF, overlapping areas WM/GM and GM/CSF, contrast ratio WM-GM and GM-CSF) are given an equal weight in this grading procedure. The crosses show the mean score and the vertical bars show the min and max scores within the subject group.

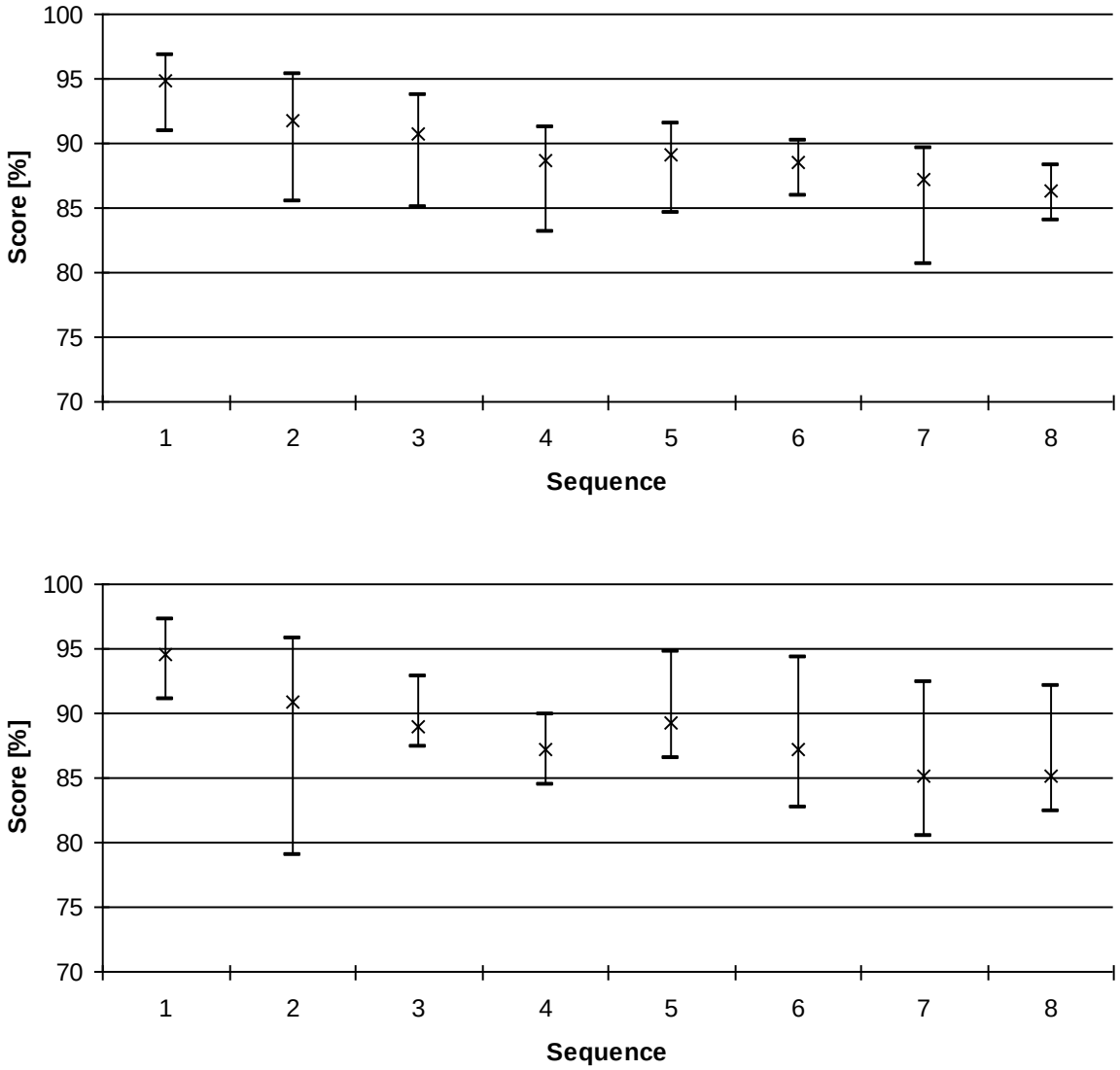

Figure 23. Results from grading of the sequences for the 12 channel coil (top) and the 32 channel coil (bottom).

A multi-way ANOVA test has been used to evaluate the variance between different sequences for both the 12- and 32 channel coils. A summary of the results from the statistical analyse is found in appendix B.

The vertical bars (in figures 25-33) denote 0.95 confidence intervals within the volunteer group. Figure 24 show the contrast ratio between WM-GM as a function of sequence for both head coils. There is a significant dependence of both the choice of head coil and sequence parameters with p-values of < 0.001.

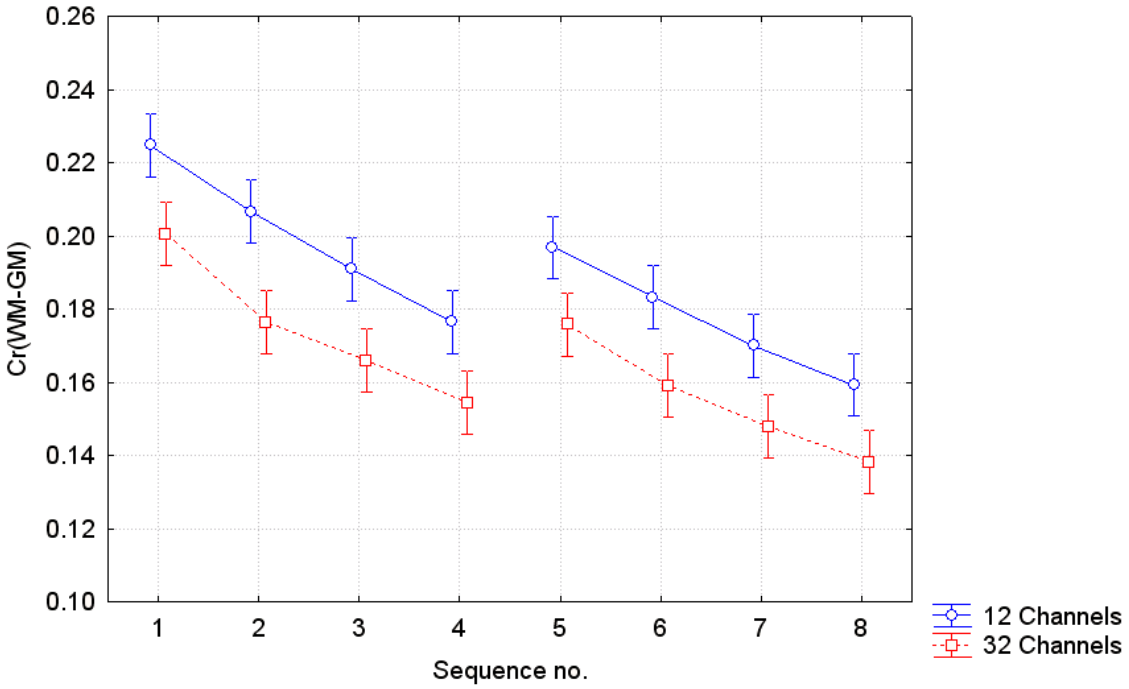

Figure 24. Contrast ratio between WM and GM for sequence 1-8.

Figure 25 show the overlapping area between WM/GM as a function of sequence for both head coils. There is a significant dependence of the choice of head coil with a p-value < 0.001. The dependence of sequence parameters is not significant (p = 0.097).

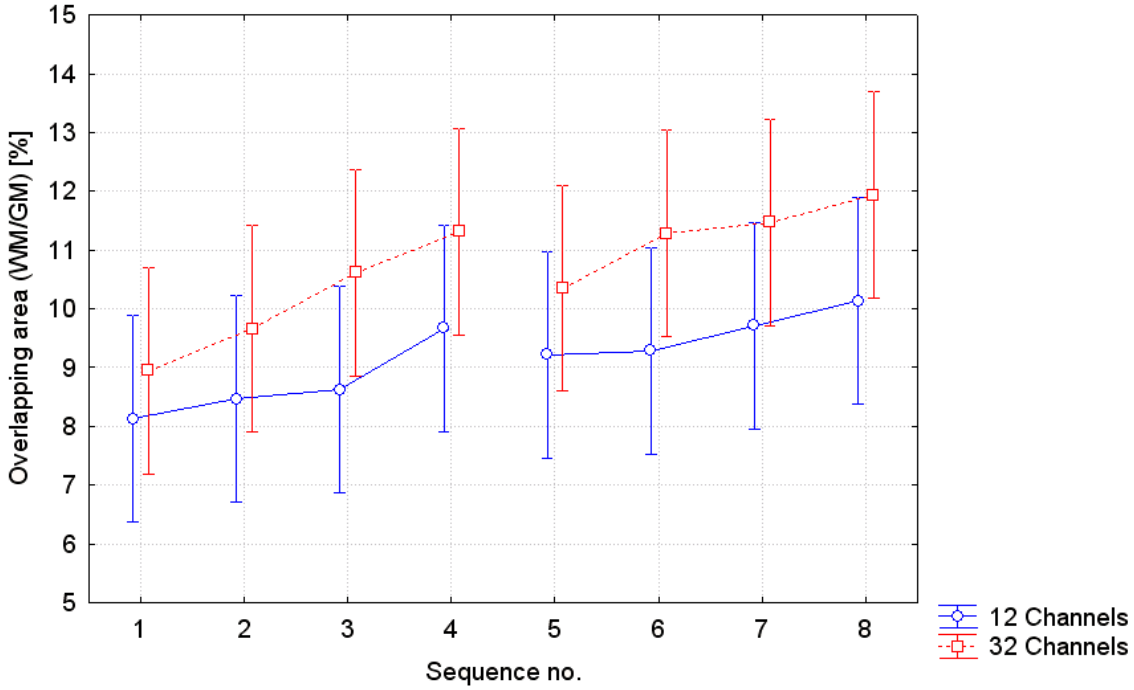

Figure 25. Overlapping area between WM and GM for sequence 1-8.

Figure 26 show CNR as a function of sequence for both head coils. CNR was calculated by dividing the difference in signal intensity between WM-GM by the standard deviation of the background signal. There is a significant difference of CNR depending of the head coil (p < 0.001). The difference of CNR as a function of sequence is not significant (p = 0.262).

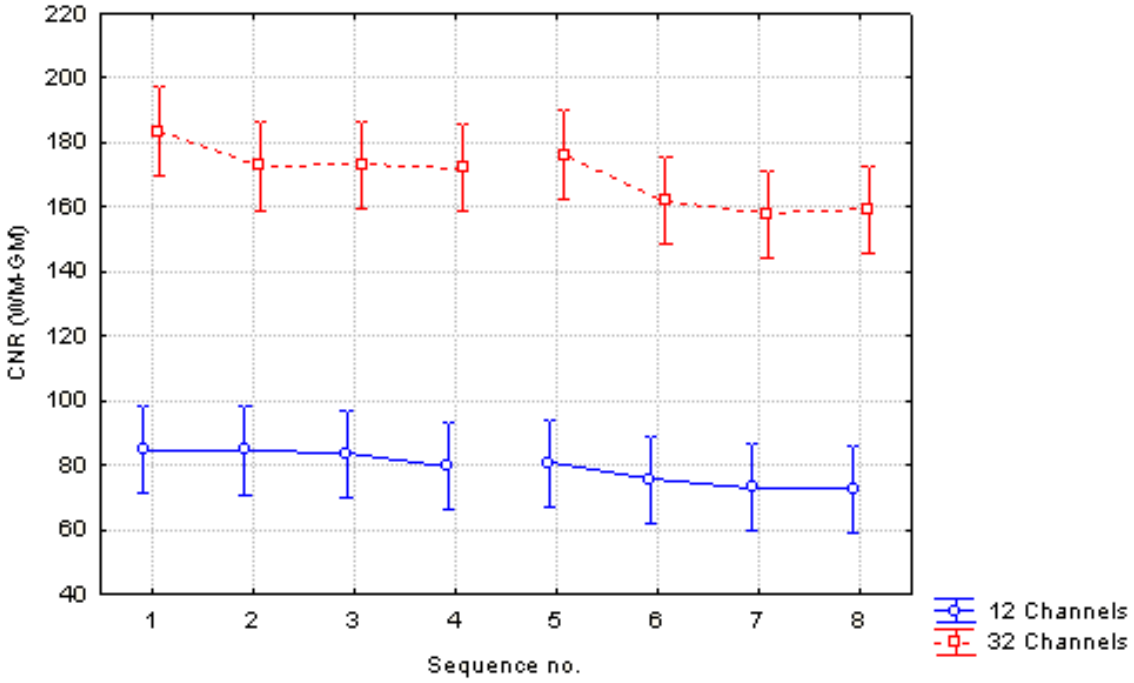

Figure 26. CNR calculated by equation 4 as a function of sequence.

Figure 27 show the contrast ratio between GM-CSF as a function of sequence for both head coils. There is a significant dependence of the choice of sequence with a p-value < 0.001. There is no significant dependence between the choice of head coil and GM/CSF contrast (p = 0.140).

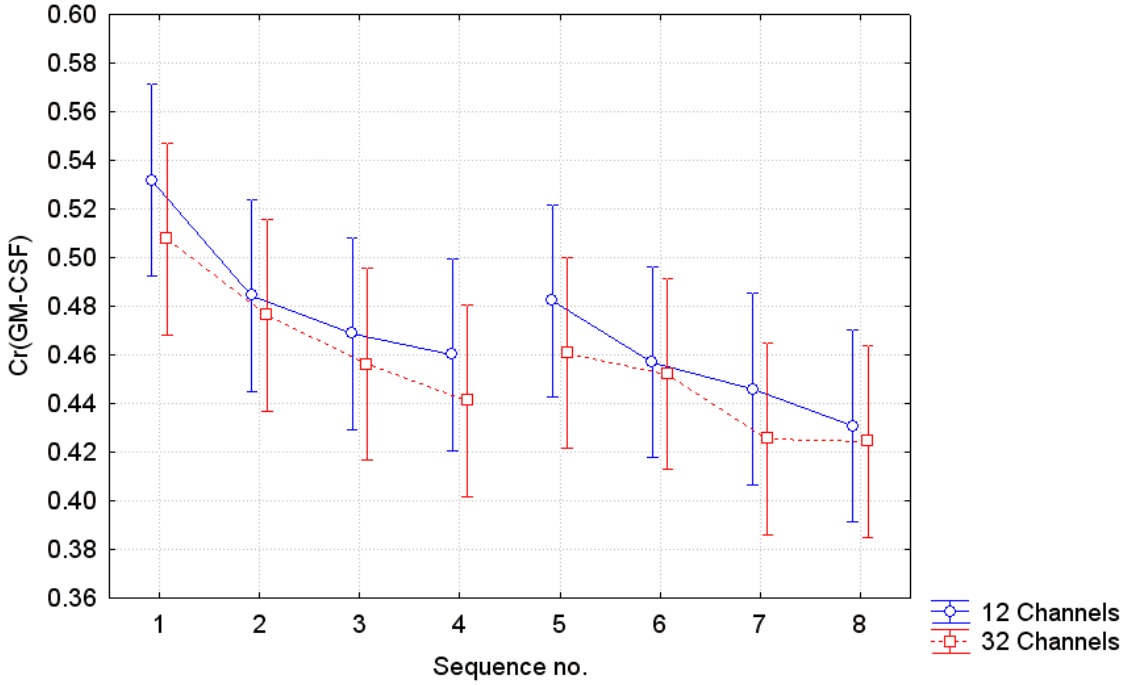

Figure 27. Contrast ratio between GM and CSF for sequence 1-8.

Figure 28 show the overlapping area between GM/CSF as a function of sequence for both head coils. There is a significant dependence of the choice of head coil (p < 0.001), but not with the choice of sequence (p = 0.350).

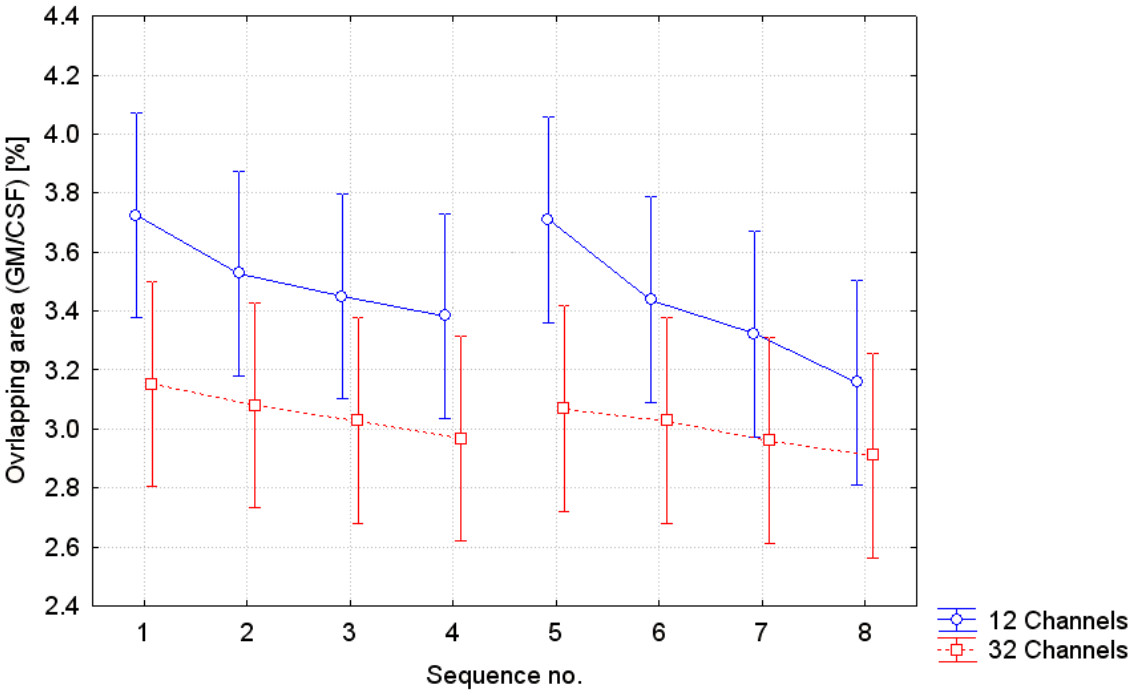

Figure 28. Overlapping area between GM and CSF for sequence 1-8.

Figure 29 show the CSF volume as a function of sequence for both head coils. There is a significant dependence of the choice of sequence with a p-value < 0.001. The dependence of head coil is not significant (p = 0.089).

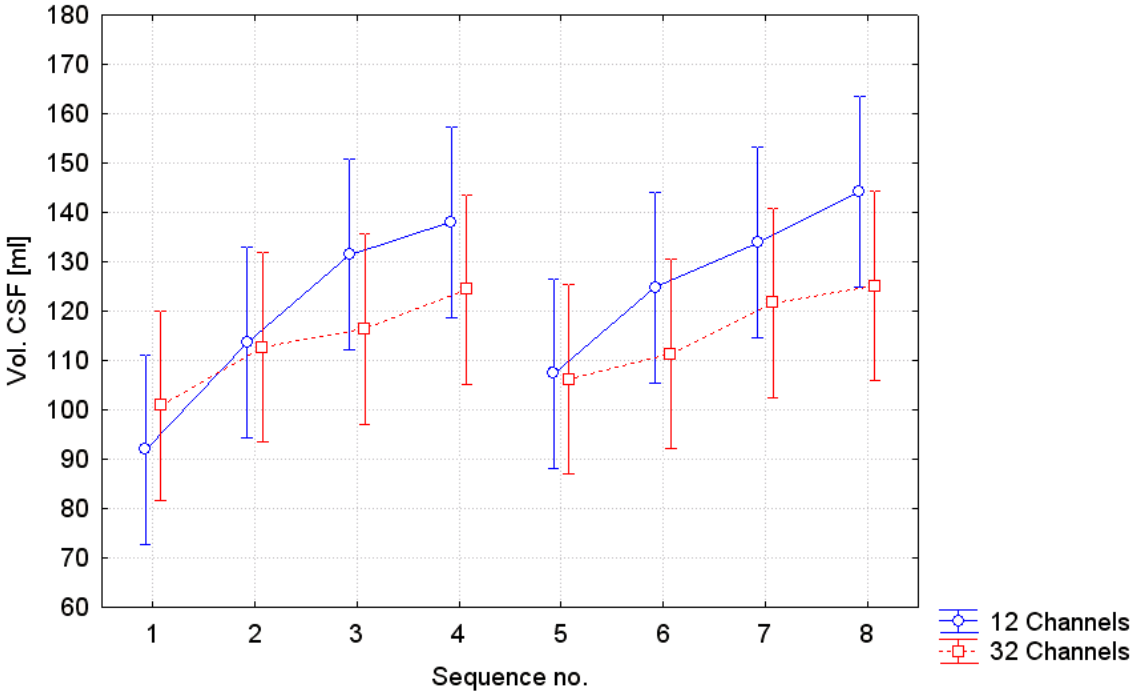

Figure 29. CSF volume for sequence 1-8.

The signal intensity of CSF is shown as a function of sequence for both head coils in figure 30. There is a significant dependence of both choice of head coil and sequence with p-values < 0.001.

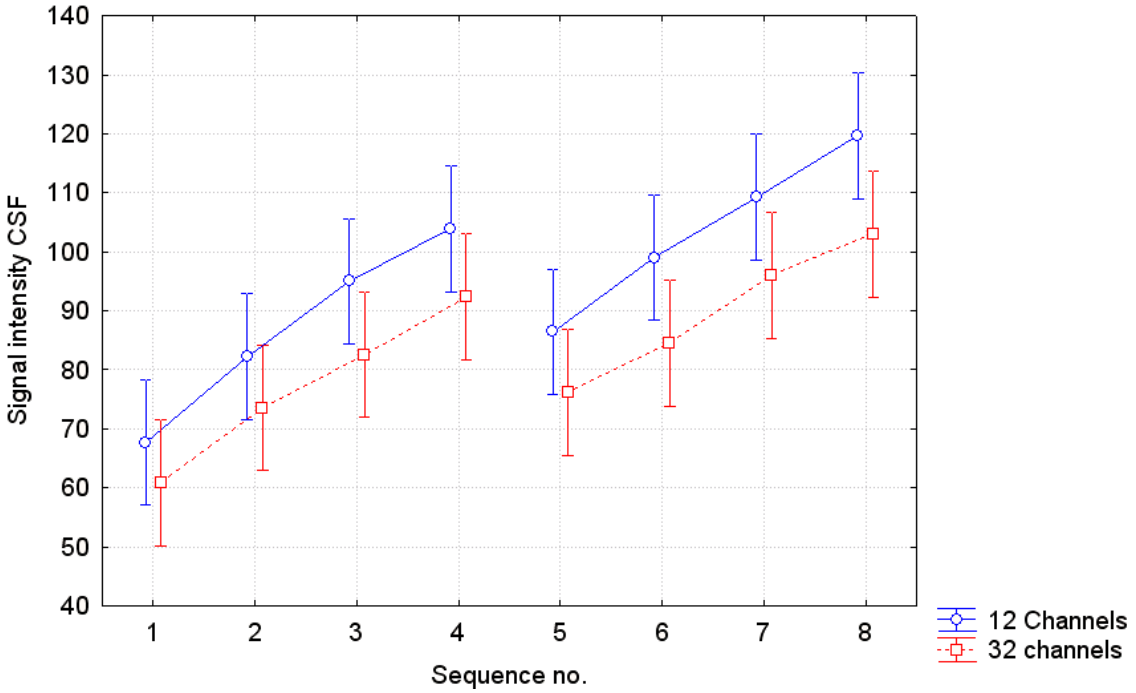

Figure 30. CSF signal intensity for sequence 1-8.

Spearmans rank correlation coefficient was calculated to investigate the correlation between CSF signal intensity and CSF volume. The correlation coefficient for the mean value of the volunteer group was 1.0 both for both head coils, sequence 1-4 and sequence 5-8.

Figure 31 show CNR as a function of sequence for both head coils. CNR is calculated by dividing the difference in signal intensity between GM-CSF by the standard deviation of the background signal. There is a significant difference of CNR depending of the head coil ($p < 0.001$). The difference of CNR as a function of sequence is not significant ($p = 0{,}062$).

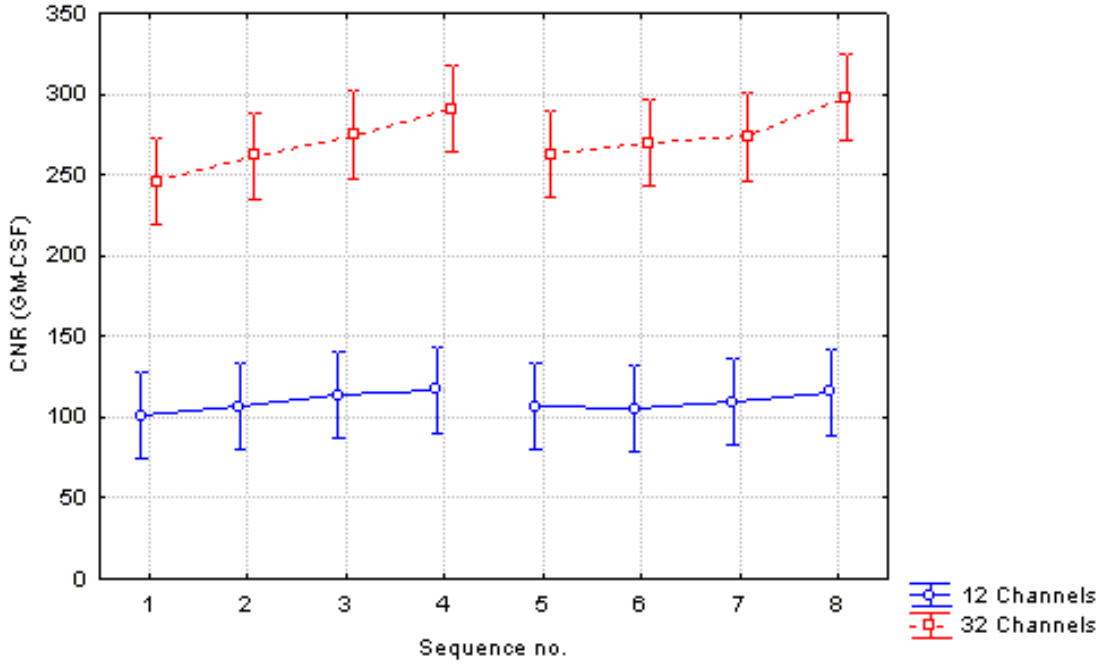

Figure 31. CNR calculated by equation 4 as a function of sequence.

Figure 32 show the Brain Parenchymal Fraction (BPF) in percent as a function of sequence for both head coils. The BPF is significantly dependent of the choice of sequence ($p = 0.020$) but not of head coil ($p = 0.700$).

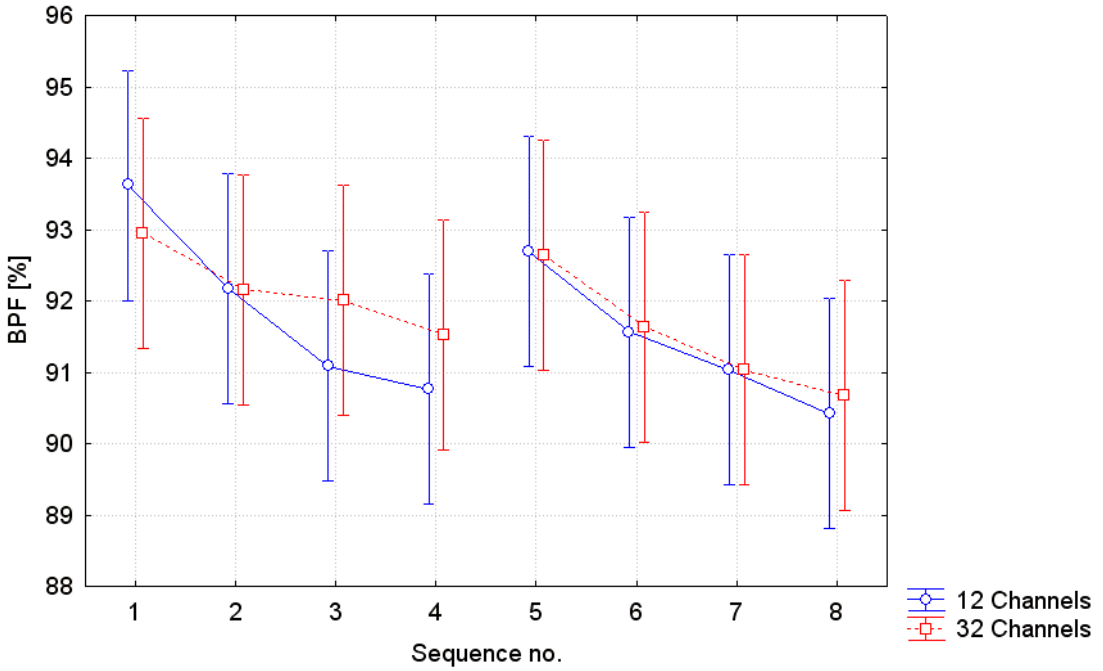

Figure 32. Brain Parenchymal Fraction (BPF) in percent for sequence 1-8.

The BPF for the 9 volunteers was 0.918 ± 0.025, range 0.865-0.971.

4.5.2 Evaluation by neuro-radiologist

The consultant neuro-radiologist could see no difference at all between images from the same coil and sequence. Images from the 32 channel coil were less noisy and more pleasant to look at than images from the 12 channel coil. In terms of clinical diagnosis there were no difference between sequence parameters or coil, all images were given grade 4, between approved and excellent. The contrast and colour scale were perceived as slightly better when TI = 800 ms was used compared to 850 ms.

4.5.3 Comparison between the 12- and 32 channel head coils

The average CNR of WM-GM and GM-CSF for all images in the volunteer study is shown for both coils in table 9.

Table 9. Average CNR of WM-GM and GM-CSF for both head coils.

	12 channel coil	32 channel coil
Average CNR WM-GM	67.0	200.3
Average CNR GM-CSF	98.4	294.3

Figure 33 shows an example of the image histograms from BMAP. The top one is from the 12 channel coil and the bottom one from the 32 channel coil. The black curve represents the original histogram. The pink curve is a fitted curve used for the gauss approximations in blue. A shift in signal intensity values can be seen between the different head coils.

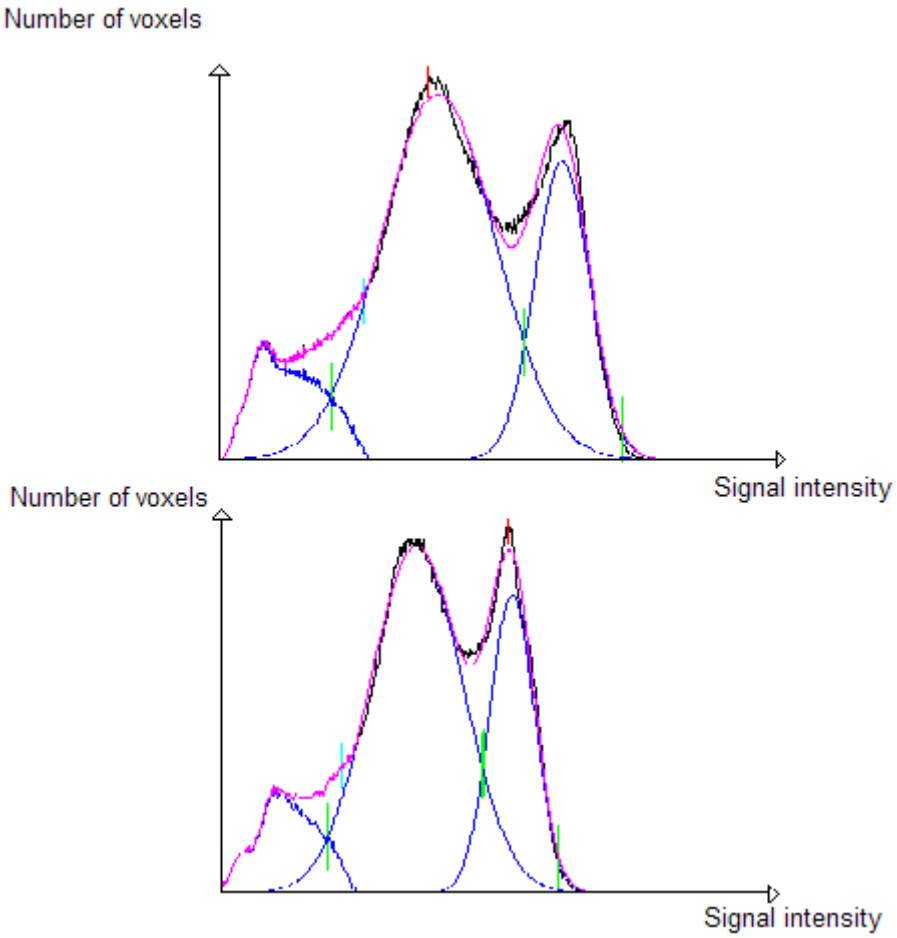

Figure 33. The upper image histogram is from a segmented brain acquired with the 12 channel coil. The bottom image histogram is from a segmented brain acquired with the 32 channel coil.

Figure 34 show the intensity profiles from two segmented brains. The image with the red intensity profile was acquired with the 12 channel coil and the image with the green intensity profile was acquired with the 32 channel coil.

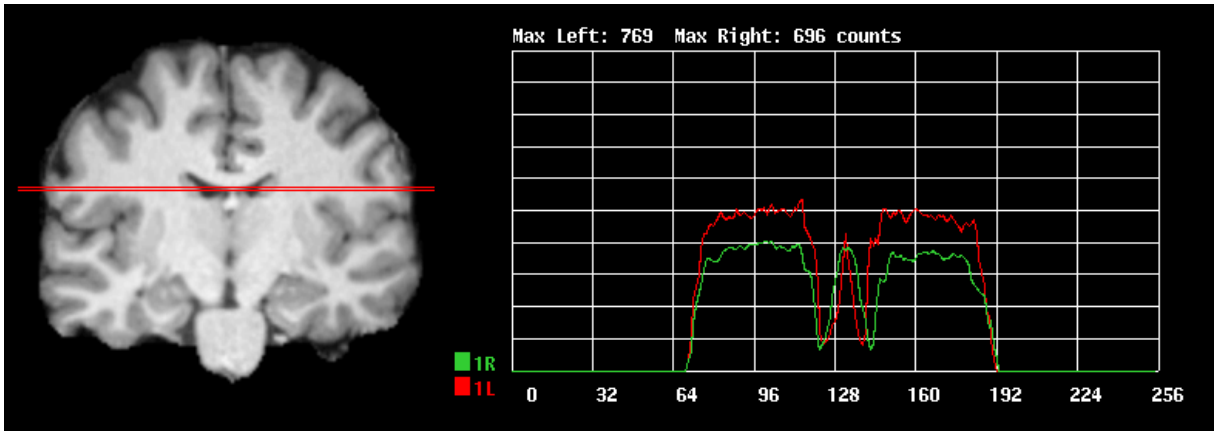

Figure 34. Intensity profiles of two segmented brains. Red profile – 12 channel coil. Green profile – 32 channel coil.

4.5.4 Repeatability study

Table 10 shows the mean volume (total, WM, GM, CSF) and mean BPF within 0.95 confidence interval and the coefficient of variation (C_v) in percent for both coils. Six images have been acquired of 1 volunteer with each coil.

Table 10. Tissue volumes and BPF with 0.95 confidence interval (± 2 standard deviations) and coefficient of variation (C_v) in percent for both coils.

	12 channel coil	32 channel coil
Mean tot. vol. [ml]	1330.3	1317,7
2SD	6.4	17.8
C_v	0.2	0.7
Mean BPF	0.93	0.90
2SD	0.01	0.07
C_v	0.5	0.4
Mean WM vol. [ml]	326.8	349.8
2SD	14.1	14.1
C_v	2.2	2.0
Mean GM vol. [ml]	908.4	840
2SD	30.5	26.0
C_v	1.7	1.5
Mean CSF vol. [ml]	95.1	127.9
2SD	13.0	9.9
C_v	6.8	3.9

Table 11 show the results from a paired t-test between the 6 images acquired with the 12 channel coil and the 6 images acquired with the 32 channel coil.

Table 11. Paired t-test between the 12- and 32 channel coils.

Parameter	p	t	Effect size
Total vol.	0.024	3.2	0.82
WM vol.	< 0.001	-8.2	0.97
GM vol.	< 0.001	9.7	0.97
CSF vol.	0.001	-7.2	0.95
BPF	0.001	7.6	0.96

Table 12 shows the results from a second repeatability study performed on a second subject to evaluate the dependence of voxel size and main magnetic field strength with the 12 channel coil. The parameters were measured and calculated from six images with each scanner/resolution combination. The mean values of the six images are shown.

Table 12. Summary of the mean results from the repeatability study with 1.5T and 3T with two different voxel sizes. The 12 channel head coil has been used for all scans.

	3T 1 mm^3	3T 2.2 mm^3	1.5T 2.2 mm^3
Cv tot. vol.	0.28	0.12	0.06
Cv WM vol.	1.52	1.96	1.06
Cv GM vol.	0.66	1.96	0.52
Cv CSF vol.	4.62	54.4	2.64
Cv BPF vol.	0.30	0.89	0.16
Peak WM	639	600	552
Peak GM	437	383	375
Peak CSF	182	156	120
P. dist. WM-GM	202	218	178
P. dist. GM-CSF	254	227	255
Cr WM-GM	0.19	0.22	0.19
Cr GM-CSF	0.41	0.42	0.51
Overl. WM/GM	8.4	26.0	9.9
Overl. GM/CSF	2.6	3.5	3.6
Tot. vol. [ml]	1572	1557	1616
Vol. WM [ml]	482	425	364
Vol. GM [ml]	991	1107	1162
Vol. CSF [ml]	98	25	90
BPF	0.94	0.98	0.94
CNR WM-GM	288	3235	181
CNR GM-CSF	413	3366	228

5 DISCUSSION

5.1 Shimming and intensity correction

The intensity profile from the spherical oil phantom acquired with automatic shimming show some minor inhomogeneities at the centre of the phantom. Table 5 shows the segmentation parameters from the image acquired with automatic- and manual shimming. The segmentation results only differs a few percent from each other. The conclusion is that manual shimming is not necessary for the outcome of the segmentation result.

At the intensity profiles from the segmented brain images with- and without intensity correction for signal inhomogeneities a decreased intensity can be seen at the base of the brain without correction. This is an effect of signal sensitivity of the head coils and B_1 inhomogeneities occurring when body size becomes significant with respect to the wavelength of the radiation transmitted due to a dielectric resonance effect. Because of these inhomogeneities, intensity correction of the images is needed to improve the brain/non-brain tissue segmentation.

5.2 Prestudy 1, MRI test objects

Figures 13 and 14 from prestudy 1 show how the contrast ratio between the test objects varies with FA and TI. The contrast ratio decreases with increasing FA and increasing TI. Since the masking process is dependent on a high contrast ratio between different brain tissues all FA larger than 10º and TI longer than 1000 ms could be removed from further studies for both head coils. The spread of Cr as a function of FA and TI was as high as 65% for the 32 channel coil and 32% for the 12 channel coil. This is an indication that the 32 channel coil is in greater need of an optimization than the 12 channel coil.

The relaxation times of the gel that is used differ from the values of WM and GM found in literature. Also the contrast ratio with CSF is not considered. Hence no further conclusions about what contrast parameters should be used can be drawn from this first study.

5.3 Prestudy 2, optimization of the mask file

The results from prestudy 2, optimization of the mask file, show that mask file number 1 is preferable. Mask file number 5 should not be used since it results in a considerably larger total volume than the other mask files. The reason for this is because it is has the lowest intensity constraints and therefore includes non-brain tissue. Small quantities of non-brain tissue can be hard to detect from a quick overview, but it quickly adds up to a considerable extra volume if it occurs on many slices of the brain. The largest difference in total volume between all mask files except for number 5 is < 2% for both sequences and coils.

It is possible to see some differences of the masking result by visual inspection. However, to perform a complete visual inspection would be too time consuming for this project since each of the 24 segmentations contains 256 slices. All slices were browsed through quickly to find out if larger amounts of non-brain tissue had been included.

The relationship between the coils is unchanged as a function of mask file. The total volume is slightly lower with the 32 channel coil for all mask files when the high contrast parameters are used. When the low contrast parameters are used this relationship is reversed, the total volume is slightly higher for the 32 channel coil. The relationships between the coils are also

the same with BPF, high contrast parameters gives lower BPF for the 32 channel coil, low contrast parameters gives higher BPF for the 32 channel coil.

5.4 Prestudy 3, Selection of scan protocol

In figures 18 and 19 it can be seen that eight different images, four from each coil, with TI = 700 ms resulted in zero or close to zero CSF volume. These results obviously derive from unsuccessful segmentations. Because the segmentation software can not manage CSF when TI of 700 ms is used, the shortest TI kept for the volunteer study was 800 ms. It can be seen that the CSF volume still varies with FA for TI = 800 ms. When TI = 900 ms the CSF volume is quite constant as a function of FA. This indicates that the segmentation software begins to treat CSF voxels more correctly with a TI somewhere between 800-900 ms.

A successful segmentation should have long peak distances between both WM-GM and GM-CSF, high contrast ratio between WM/GM and GM/CSF and small overlapping areas between WM/GM and GM/CSF. The plots showing peak distance (figure 20), Cr (figure 21) and overlapping area (figure 22), all suggest that small FA and short TI give a better segmentation result. These plots however only show the relationship between WM and GM. Before more information about CSF is available the scan protocol should not be too specific. It is however reasonable from these results that FA = 10º can be removed from the scan protocol because of its low WM/GM contrast. It was also obvious from the first volunteer that FA = 11° resulted in too low WM/GM contrast. Since this trend of decreasing contrast with increasing FA was evident, one volunteer was considered enough to remove FA = 11° from the scan protocol of the second volunteer in order to save time.

5.5 Volunteer study

5.5.1 Optimization of contrast parameters

Figure 23 shows the result from the grading of the sequences for both head coils. There is a trend in these figures which indicates that short TI gives a higher score. Sequence 1 gets the best result for both coils and should be the optimal sequence for automatic segmentation of brain tissue if this grading system was adequate. To be certain of this result, a statistical analysis of some different parameters was needed.

The contrast ratio between WM/GM is increasing with decreasing TI (figure 24). The overlapping area between WM/GM is decreasing with decreasing TI (figure 25). The variation of the overlapping area is insignificant as a function of sequence, probably because there is such large variation within the subject group. The CNR of WM-GM is higher for shorter TI, but this relationship is not significant (figure 26). When just looking at WM and GM there is no doubt that FA = 8° and TI = 800 ms is the best choice of image contrast parameters.

For a successful segmentation however, CSF also has to be considered. In figure 27 it can be seen that Cr between GM/CSF is increasing with decreasing TI. The overlapping area between GM/CSF (figure 28) is also increasing with decreasing TI, but this relationship was found to be insignificant. In figure 29 it is shown that the CSF volume depends on the sequence, more particularly, the CSF volume depends on TI. Short TI results in a small CSF volume. Figure 30 show increasing signal intensity with increasing TI. A conclusion of figures 29 and 30 is that higher signal intensity for CSF result in a larger CSF volume, hence high signal intensity for CSF is wanted. This explains why a high Cr between GM-CSF gives a small CSF volume. The CNR of GM-CSF is higher for longer TI, but the significance as a function of sequence is low (figure 31).

Two different studies have been found where BPF has been measured with 1.5 T MRI units. The first study by Bermel et al. contains a healthy control group of 17 patients (13 women, 4 men, age 24-57 years). The BPF was measured by a semi automated method to 0.877 ± 0.020, range 0.835-0.901 [22]. The second study by Kassubek et al. contains a healthy control group of 70 patients (25 women, 45 men, age 21-76). The BPF was measured using largely automated methods to 0.8281 ± 0.0368, range 0.7300-0.8837 [23].

Figure 32 show the BPF from this study in percent. BPF is increasing with decreasing TI because the CSF volume is decreasing with decreasing TI. As shown in previous studies, the high BPF values from sequence 1 are not likely to be true. Sequence 2 is a better choice since it results in a larger CSF volume and therefore lower, and likely more realistic, BPF. A first attempt of the repeatability study was conducted with sequence 1. This attempt resulted in an average BPF of 0.975 and an average CSF volume of 35.35 ml which is not likely for a healthy male subject of age 27.

In prestudy 3 it was shown that the optimal sequence for automatic volumetry should have TI in the range of 800-900 ms to get good segmentation result of WM, GM and CSF. Even though sequence 1 had the best properties of WM/GM when it comes to contrast, peak distance and overlapping area, it was not good enough for CSF segmentation. Sequence 2 was therefore chosen as the optimal sequence for the repeatability study.

These results suggests that the histogram parameters evaluated (peak distance, overlapping area and Cr) are not sufficient for evaluation of the CSF segmentation. A reason for this may be that the CSF peak sometimes is hard to distinguish in the image histogram, and no gauss approximation is made for the CSF volume. Based on the data available from this study a compromise had to be made between the histogram parameters and the most realistic CSF result.

5.5.2 Evaluation by neuro-radiologist

The consultant neuro-radiologist found all images acceptable in terms of tissue contrast for clinical diagnosis. The images from the 32 channel coil were more pleasant to look at when no window settings were made. They were also less noisy. The images with TI = 800 ms were preferable to those with TI = 850 ms, probably because of the slightly higher WM-GM contrast. The relative contrast between GM-CSF is considerably higher than the relative contrast between WM-GM for all contrast parameters that has been viewed.

5.5.3 Comparison between the 12- and 32 channel head coils

When comparing the different coils it can be seen that C_v (from the repeatability study) for the total volume is smaller with the 12 channel coil. The coefficients of variation for WM-, GM-, CSF volume and BPF are smaller with the 32 channel coil. This indicates that the 32 channel coil give more reproducible results than the 12 channel coil, but the differences are so small that more data would be needed to see if they are significant.

The paired t-test shows that there is a small significance between the total volume and the choice of coil with a large effect size. A large effect size (≥ 0.8) means that the significance is relevant to the sample group. For the WM-, GM-, CSF volume and BPF there is a highly significant difference with the choice of head coil. It can also be seen in table 11 from the negative t-values that the 12 channel coil underestimates the WM- and CSF volumes in comparison to the 32 channel coil. This conclusion however also needs more data to be proven significant since sequence 2 approximately results in the same CSF volume for both

coils in figure 29, and the same BPF in figure 32 from the main volunteer study with 9 subjects.

Figure 33 show the image histograms for both the 12- and 32 channel coils. The histogram from the 32 channel coil has a slightly lower intensity range. Figure 34 show intensity profiles from two segmented brains, one acquired with each coil. The red intensity profile from the 12 channel coil has a higher signal value for WM, and approximately the same signal value for CSF. The conclusion from these images is that the intensity range is smaller with the 32 channel coil, which explains why the contrast ratio between WM-GM is smaller with this coil. The reason for this may be due to different coil sensitivities. The size of the coil elements can cause non-uniformity, as well as interaction in reception sensitivity between the elements. Another reason could be the intensity correction in the image post processing. The intensity correction used in BMAP is developed with images from 1.5 T and could probably be improved for both the 12- and 32 channel head coil at 3 T.

The comparison between the two different head coils speaks much in favour of the 12 channel coil. The contrast ratio between WM-GM is significantly higher with the 12 channel coil. The WM/GM overlapping areas are significantly smaller with the 12 channel coil. There is an indication of a better GM-CSF contrast with the 12 channel coil, even though this difference is not statistically significant. When it comes to the overlapping area between GM/CSF the 12 channel coil is the better choice again. The BPF is approximately the same with both coils when sequence 2 is used. The first thing that speaks in favour of the 32 channel coil is the decreased noise level. SNR is hard to measure in images acquired with parallel imaging since the noise is not homogenously distributed over the volume. Instead the standard deviation of the background signal was measured and compared. This standard deviation was 3.5 times higher with the 12 channel coil than with the 32 channel coil. Figures 26 and 31 shows the CNR for WM-GM and GM-CSF respectively. The average CNR (WM-GM and GM-CSF) for all sequences is 3 times higher with the 32 channel coil (table 12). This increased noise with the 12 channel coil does however not seem to have any detrimental effects on the segmentation.

5.5.4 Repeatability study

The results of the first repeatability study are shown in tables 10 and 11. The coefficients of variation for the total volume and BPF are $\leq 0.7\%$ with both coils. For WM, GM and CSF C_v is larger, in the range of 1.5 – 6.8% for the different tissue types.

In a previous study by Watson et al. [24] the repeatability was tested on a 1.5T MRI unit with a voxel size of 2.2 mm^3 using BMAP and FSL as segmentation tools. The results (C_v) from this study are shown in table 13.

Table 13. C_v in percent from a study by Watson et al. (2006) on a 1.5T MRI unit.

	C_v (BMAP)	C_v (FSL)
Mean tot. vol.	0.02	0.9
Mean vol. WM	0.8	0.9
Mean vol. GM	0.4	0.8
Mean vol. CSF	1.1	3.2
Mean BPF	0.3	0.5

The results were better with BMAP than FSL, C_v is 45 times smaller for the total volume and almost 3 times smaller for the CSF volume. The coefficient of variation for the total volume is

10 times smaller than in this study. One explanation for this is that the mask created for the first brain was used on all images. In this study a new mask was created for each brain. The coefficient of variation was 2 – 6 times smaller for the specific brain tissue volumes and slightly smaller for BPF in the previous study when BMAP was used. Because of these impaired results the repeatability was tested again with a new test subject and the 12 channel coil. Two different voxel sizes were used (1 mm^3 and 2.2 mm^3). For comparison with the previous study a 1.5T MRI unit was also used (MAGNETOM Avanto, Siemens, Medical Solution, Erlangen, Germany) with the larger voxel size. In this second attempt the results from the 3T MRI unit were slightly improved (see table 12). When the larger voxel size (2.2 mm^3) was used with the 3T MRI unit, the resulting CSF volume was unrealistically low. The reason for this is still unknown, but it could be an effect of B_1 inhomogeneities at 3T. The 1.5T MRI unit treats CSF more correctly with 2.2 mm^3 voxel size which excludes partial volume effects as an explanation.

The results with the 1.5T MRI unit were almost the same as in the previous study which indicates that the different results from these studies are not a function of the segmentation procedure, but rather a function of field strength. It is however possible that the segmentation procedure and intensity correction can be further optimized for images acquired with the 3T MRI unit to improve the repeatability.

With increased field strength, the WM- and CSF volume is increasing, while the GM volume is decreasing. This indicates that WM and CSF may be classified as GM with a lower field strength, which may explain the larger overlapping area for 1.5T.

The conclusions of this repeatability study are that when the voxel size is increased at 3T, the segmentation of CSF fails. This might be an effect of B_1 inhomogeneities since the same problem is not seen at 1.5T. It might be possible to improve the intensity correction in BMAP to reduce this problem.

The coefficient of variation is lower at 1.5T for the total volume, WM volume, GM volume, CSF volume and BPF. The signal intensity values are increasing with increasing field strength.

6 CONCLUSIONS & FUTURE WORK

The contrast parameters chosen for brain tissue segmentation from the optimization are FA = 8° and TI = 850 ms for both the 12- and 32 channel head coils. These parameters gave the best result when all aspects of the segmentation were considered. The results however show that the image histogram parameters; peak distance, overlapping area and Cr are not sufficient for evaluating the segmentation result of CSF. A compromise had to be made between a realistic segmentation result for CSF and the histogram parameters of WM and GM.

The consultant neuro-radiologist gave all images the score 4 on a scale where 5 corresponds to excellent image quality. The images acquired with the 32 channel coil were perceived as more pleasant to look at, but the anatomical information was the same with both coils. The WM tissue was considered too bright with the 12 channel coil when no window settings were set.

The comparison between the 12- and 32 channel head coils show that there is no specific advantage of using a 32 channel coil for segmentation purposes. The 32 channel coil gives less noise and higher CNR in the images but this does not seem to have any detrimental effect on the segmentation result. Nearly all statistical tests of the evaluated parameters show a significant dependence with choice of head coil. Of the six parameters used for the sequence evaluation (contrast ratio, peak distance and overlapping area between WM-GM and GM-CSF) the 12 channel coil was significantly better at four. The 32 channel coil had a smaller overlapping area between GM/CSF and there was no significant dependence of the GM-CSF contrast ratio as a function of coil (appendix B). Overall the 12 channel coil is the best choice for brain tissue segmentation when looking at these parameters.

The results from the repeatability study were a little bit worse than expected. The variation in total brain volume and BPF was small ($C_v \leq 0.7$), and the variation of the WM-, GM-, and CSF volumes was acceptable. The repeatability results however were not as good as in a previous study on a 1.5T MRI unit. Since these results on the 1.5T MRI unit was repeated in this study the difference is probably a function of field strength rather than segmentation procedure. It may however be possible to further optimize the segmentation for 3T. Since B_1 inhomogeneities is one likely explanation for the impaired repeatability results it would be a good start to modify the intensity correction in BMAP. The intensity shift as a function of field strength indicates that a modification of the intensity intervals in the mask file also may improve the segmentation results at 3T.

The images acquired in this project will be used for manual tracing of the putamen and hippocampus. The differences between manual and fully automatic segmentations in regional volumetry can be evaluated as a function of image contrast and choice of head coil. The impaired repeatability results at 3T also need further investigation.

ACKNOWLEDGEMENTS

First of all I would like to thank my supervisor Terri Lindholm for giving me the great opportunity to work with this project, and all the excellent help and support. I would also like to thank Leif Svensson for taking time to guide me through BMAP and discuss the segmentation methodology. Eva Örndahl for all the technical support at SMILE and great input on all sorts of questions. Susanne Müller for taking time to evaluate the images. Jeffrey Looi for discussions about statistics and future work.

Finally I would like to thank all the staff at the Department of Diagnostic Medical Physics, Huddinge, for the great support and rewarding discussions. Last but not least, thanks to all volunteers who have taken their time to contribute to this project.

REFERENCES

1 Michael Grundman, Ronald C. Petersen, Steven H. Ferris, et al. (2004). *Mild Cognitive Impairment Can Be Distinguished From Alzheimer Disease and Normal Aging for Clinical Trials.* Arch Neurol. 61;59-66.

2 Clifford R. Jack Jr, Matt A. Bernstein, Nick C. Fox, et al. (2008). *The Alzheimer's Disease Neuroimaging Initiative (ADNI): MRI Methods.* Journal of Magnetic Resonance Imaging. 27:685-691.

3 Nick C Fox, Jonathan M Schott (2004). *Imaging cerebral atrophy: normal ageing to Alzheimer's disease.* The Lancet. Vol 363. Januari 31.

4 R. Deichmann, C.D. Good, O.Josephs, et al. (2000). *Optimization of 3-D MP-RAGE Sequences for Structural Brain Imaging.* NeuroImage 12, 112-127.

5 Donald W. McRobbie, Elizabeth A. Moore, Martin J. Graves, Mertin R. Prince (2003). *MRI From Picture to Proton*. Second edition (2007). New York: Cambridge University Press. ISBN: 10 0-521-68384-x.

6 Matt A. Bernstein, PhD. Kevin F. King, PhD. Xiaohong Joe Zhou, PhD. 2004. *Handbook of MRI Pulse Sequences.* Burlington: Elsiver Academic Press. ISBN: 0-12-092861-2.

7 Leif A Svensson, personal communication, 2009.

8 Ugo Salvolini, Tommaso Scarabino (2006). *High Field Brain MRI*. Berlin Heidelberg: Springer-Verlag. ISBN: 3-540-31775-9.

9 Stephen M. Smith (2002). *Fast Robust Automated Brain Extraction.* Human Brain Mapping. 17:143-155.

10 Smith S.M., Jenkinson M., Woolrich M.W. Beckmann C.F., et al. (2004). *Advances in functional and structural MR image analysis and implementation as FSL*. NeuroImage 23 S208-S219.

11 Yongyue Zhang, Michal Brady, Stephen Smith (2001). *Segmentation of Brain MR Images Through a Hidden Markov Random Field Model and the Expectation-Maximization Algorithm*. IEEE. Transactions on Medical Imaging vol. 20, no. 1.

12 Stephen M. Smith, Anil Rao, Nicola De Stefano, et al. (2007). *Longitudinal and cross-sectional analysis of atrophy in Alzheimer's disease: Cross-validation of BSI, SIENA and SIENAX.* Academic Press. Neuroimage, 36 1200-1206.

13 Marco Battaglini, Stephen M. Smith, Susanna Brogi, Nicola De Stefano (2007). *Enhanced brain extraction improves the accuracy of brain atrophy estimation.* NeuroImage 40 S583-S589.

14 Koen Van Leemput, Frederik Maes, Dirk Vandermeulen, Paul Suetens (1999). *Automated Model-Based Tissue Classification of MR Images of the Brain.* IEEE. Transactions on Medical Imaging, vol. 18, no. 10.

15 Frederik Maes, André Collignon, Dirk Vandermeulen, Guy Marchal, Paul Suetens (1996). *Multi-Modality Image Registration by Maximization of Mutual Information.* IEEE. Mathematical Methods in Biomedical Image Analysis. S14-S22.

16 David J. Larkman, Rita G. Nunes (2007). *Parallel magnetic resonance imaging.* Physics in medicine and biology 52. R15-R55.

17 S.O Shoenberg, O. Dietrich, M. F. Reiser (2007). *Parallel Imaging in Clinical MR Applications.* Berlin Heidelberg: Springer-Verlag. ISBN: 3-540-23102-1

18 Mark A. Griswold, Peter M. Jakob, Robin M. Heidemann et al. (2002). *Generalized Autocalibrating Partially Parallel Acquisitions (GRAPPA).* Magnetic Resonance in Medicine 47:1202-1210.

19 Terri L. Lindholm, Lisa Botes, Eva-Lena Engman et al. (in review, 2009). *Parallel Imaging: Is GRAPPA a useful acquisition tool for MR imaging intended for volumetric brain analysis?* BMC Medical Imaging.

20 Nakumura Masanobu, Ikeda Nobuhiro, Tsuboko Toshikazu et al. (2006). *Clinical Usage of Parallel Imaging of Head Three-dimensional MR Image for Analysis of VSRAD: A Comparison of Imaging Statistical Analytic Results in SENSE Acquisition Method Shortening Acquisition Time Versus Conventional Acquisition Method.* Japanese Journal of Radiological Technology. VOL.62;NO.10;PAGE.1456-1462.

21 Janaka P. Wansapura, PhD, Scott K. Holland, PhD, R. Scott Dunn, RT, and William S. Ball, Jr., MD. 1999. *NMR Relaxation Times in the Human Brain at 3.0 Tesla*. Journal of Magnetic Resonance Imaging 9:531-538.

22 Robert A. Bermel, Jitendra Sharma, Christopher W. Toja et al. (2003). *A semiautomated measure of whole brain atrophy in multiple sclerosis.* Journal of the Neurological Sciences 208. 57-65.

23 Kassubek Jan, Bernhard Landwehrmeyer G., Ecker Daniel et al. (2004). *Global cerebral atrophy in early stages of Huntington's disease: quantitative MRI study.* NeuroReport vol. 15(2). 363-365.

24 T. L. Watson, T. Jonsson, L. Botes et al. *Magnetic Resonance Paralell Imaging in the Evaluation of Brain Volumes.* International Conference on Alzheimer's Disease, 2006.

APPENDIX A

List of mask file settings

Mask file 1

Action	Lower level [%]	Upper level [%]	Connection criteria	Loop
G_1-1	70	100	2	200
G_1-2	60	70	4	200
G_1-3	55	60	5	8
G_1-4	50	55	6	200
G_1-5	40	50	7	200
G_1-6	-	-	-	-
Restore MR		√		
G_1-7	-	-	-	-
G_2-1	40	-	4	10
G_2-2	1	-	4	10
G_2-3	1	-	8	80
Fill map	-	-	-	20
Smooth map	43	-	-	10
Grow erode	-	-	-	4

Mask file 2

Action	Lower level [%]	Upper level [%]	Connection criteria	Loop
G_1-1	70	100	2	200
G_1-2	60	70	4	200
G_1-3	55	60	5	8
G_1-4	50	55	6	200
G_1-5	40	50	7	200
G_1-6	**30**	**40**	**7**	**200**
Restore MR		√		
G_1-7	-	-	-	-
G_2-1	40	-	4	10
G_2-2	1	-	4	10
G_2-3	1	-	8	80
Fill map	-	-	-	20
Smooth map	43	-	-	10
Grow erode	-	-	-	4

Mask file 3

Action	Lower level [%]	Upper level [%]	Connection criteria	Loop
G_1-1	70	100	2	200
G_1-2	60	70	4	200
G_1-3	55	60	5	8
G_1-4	50	55	6	200
G_1-5	40	50	7	200
G_1-6	**25**	**40**	**7**	**200**
Restore MR		√		
G_1-7	-	-	-	-
G_2-1	40	-	4	10
G_2-2	1	-	4	10
G_2-3	1	-	8	80
Fill map	-	-	-	20
Smooth map	43	-	-	10
Grow erode	-	-	-	4

Mask file 4

Action	Lower level [%]	Upper level [%]	Connection criteria	Loop
G_1-1	70	100	2	200
G_1-2	60	70	4	200
G_1-3	55	60	5	8
G_1-4	50	55	6	200
G_1-5	40	50	7	200
G_1-6	**20**	**40**	**7**	**200**
Restore MR		√		
G_1-7	-	-	-	-
G_2-1	40	-	4	10
G_2-2	1	-	4	10
G_2-3	1	-	8	80
Fill map	-	-	-	20
Smooth map	43	-	-	10
Grow erode	-	-	-	4

Mask file 5

Action	Lower level [%]	Upper level [%]	Connection criteria	Loop
G_1-1	70	100	2	200
G_1-2	60	70	4	200
G_1-3	55	60	5	8
G_1-4	50	55	6	200
G_1-5	40	50	7	200
G_1-6	**20**	**40**	**7**	**200**
Restore MR		√		
G_1-7	**20**	**40**	**7**	**200**
G_2-1	40	-	4	10
G_2-2	1	-	4	10
G_2-3	1	-	8	80
Fill map	-	-	-	20
Smooth map	43	-	-	10
Grow erode	-	-	-	4

Mask file 6

Action	Lower level [%]	Upper level [%]	Connection criteria	Loop
G_1-1	70	100	2	200
G_1-2	60	70	4	200
G_1-3	55	60	5	8
G_1-4	50	55	6	200
G_1-5	40	50	7	200
G_1-6	**25**	**40**	**7**	**200**
Restore MR		√		
G_1-7	**30**	**40**	**7**	**200**
G_2-1	40	-	4	10
G_2-2	1	-	4	10
G_2-3	1	-	8	80
Fill map	-	-	-	20
Smooth map	43	-	-	10
Grow erode	-	-	-	4

The values in bold indicates criteria that have been changed from mask file 1. Mask file 5 and 6 has a *grow-mr* step after *restore MR* which was added in an attempt to include white- and grey matter cut away by the brain template.

APPENDIX B

Summary of the statistical analyse

Parameter	p(coil)	Best coil when p(coil) < 0.001	p(sequence)
Cr (WM-GM)	< 0.001	12 channel	< 0.001
Cr (GM-CSF)	0.144	-	< 0.001
Peak distance (WM-GM)	< 0.001	12 channel	0.622
Peak distance (GM-CSF)	< 0.001	12 channel	0.114
Overlapping area (WM/GM)	< 0.001	12 channel	0.097
Overlapping area (GM/CSF)	< 0.001	32 channel	< 0.001
SI(WM)	< 0.001	12 channel	0.015
SI(GM)	< 0.001	12 channel	< 0.001
SI(CSF)	< 0.001	12 channel	< 0.001
CNR (WM-GM)	< 0.001	32 channel	0.262
CNR (GM-CSF)	< 0.001	32 channel	0.062
BPF	0.700	-	0.020
Tot. vol.	0.213	-	0.968
WM vol.	0.158	-	0.022
GM vol.	0.964	-	0.103
CSF vol.	0.089	-	0.001

APPENDIX C

Svensk populärvetenskaplig sammanfattning

Love Nordin

Optimering av metod för att bestämma hjärnans volym

Demenssjukdomar är den fjärde största gruppen folksjukdomar i Sverige. I takt med att antalet äldre ökar i samhället ökar även antalet personer som drabbas av demenssjukdomar kraftigt. Ungefär var fjortonde svensk över 65 år lider av en demenssjukdom, i åldrarna över 90 år är andelen närmare hälften. Den vanligaste typen av demenssjukdom är Alzheimers sjukdom som står för ungefär hälften av alla fall. En följd av många demenssjukdomar är att nervcellerna i hjärnan förtvinar. Vid normalt åldrande sker också en minskning av hjärnvävnad som uppgår till ca 10 % från att man är fullvuxen. För en person med Alzheimers sjukdom är minskningen upp till 40 %. Ett sätt att identifiera demenssjukdomar i ett tidigt stadium är att upptäcka dessa onormala volymförändringar av hjärnan.

MRT (Magnet Resonans Tomografi) som blir en allt vanligare metod inom vården är utmärkt för att mäta hjärnans volym. En fördel med MRT är att metoden använder sig av magnetiska fält och radiovågor för att generera den signal som bygger upp bilderna, ingen joniserande strålning används. Den största fördelen med MRT är dock att man kan få en mjukdelskontrast som är överlägsen andra bildtagningsmetoder. Mjukdelskontrasten gör det möjligt att skilja olika typer av hjärnvävnad från varandra samt att kunna urskilja olika strukturer i hjärnan. Detta gör det möjligt att bestämma volymen för en viss typ av vävnad, eller en viss region av hjärnan.

Det här projektet har gått ut på att optimera bildkontrasten för att med en automatisk metod kunna bestämma hjärnans volym. För att bilderna ska kunna användas till att spåra sjukliga volymförändringar måste resultaten vara pålitliga. För att upptäcka dessa volymförändringar jämförs bilder tagna vid två olika tillfällen.

MR kameran som användes i studien har den starkaste fältstyrka som förekommer vid kliniskt bruk idag. En hög fältstyrka ger möjlighet till bilder med hög upplösning och lite brus. Genom att variera två olika parametrar i sekvensen kan kontrastförhållandena mellan hjärnans olika vävnadstyper förändras. En volontärstudie som omfattade nio unga friska personer genomfördes för att kunna utföra optimeringen. Efter att de optimala bildtagningsparametrarna valts undersöktes även repeterbarheten av volymbestämningen på en tionde volontär genom upprepade bildinsamlingar med den optimerade sekvensen.

Resultatet från projektet visar att det är möjligt att genomföra noggranna mätningar av hjärnans volym efter optimeringen. En fördel är att metoden är mycket snabb jämfört med manuella mätningar där hjärnans strukturer måste ritas in för hand. Resultaten blir även objektiva eftersom variationer som beror på personen som utför den manuella mätningen undviks.

Handledare: **Terri Lindholm** (Diagnostisk sjukhusfysik, Karolinska Universitetssjukhuset Huddinge)
Examensarbete 30 hp i Medicinsk strålningsfysik, Vt 2009
Institutionen för kliniska vetenskaper, Avdelningen för radiofysik, Lunds Universitet

APPENDIX D

Abstract till röntgenveckan, Jönköping 2009

TITEL: EN STUDIE AV BILDKONTRAST MED MPRAGE FÖR EN 12- OCH EN 32 KANALS HUVUDSPOLE PÅ ETT 3T SYSTEM: OPTIMERING FÖR AUTOMATISK VOLYMETRI AV HJÄRNAN

YRKESKATEGORI: SJUKHUSFYSIK

KEYWORDS: MPRAGE, AUTOMATISK SEGMENTERING, 3T, KONTRAST PARAMETER, VOLYMETRI, 12 VS 32 KANAL

Erlandsson Nordin L.P.1, Svensson L.A.1, Müller S.2 and Lindholm T.1
1.Universitetssjukhuset Huddinge, Diagnostisk Sjukhusfysik, Stockholm, Sverige
2.Universitetssjukhuset Huddinge, Röntgenkliniken, Stockholm, Sverige

lovenordin@gmail.com

Syfte
Regionala eller globala volymer av hjärnan är av intresse inom ett antal olika forskningsprojekt, inte minst inom Alzheimersforskning. Det här projektet går ut på att optimera MPRAGE sekvensen för att uppnå en automatisk och repeterbar segmentering av hjärnan. Volymen beräknas för hela hjärnan, grå- och vit hjärnsubstans samt cerebrospinalvätskan.

Material och metoder
MPRAGE (Magnetization Prepared Rapid Acquisition by Gradient Echo) är en T1-viktad 3D sekvens med hög upplösning som visar detaljerad anatomi i hjärnan. På grund av den höga upplösningen och hög T1 kontrast är sekvensen ett lämpligt val för segmentering av hjärnvävnad. Till segmenteringen används Brain Map Statistics som är en lokalt utvecklad programvara. De parametrar i sekvensen som varieras för att uppnå olika kontrastförhållanden är flippvinkel och inversionstid. Flippvinklar på 8-11º undersöks för olika inversionstider i intervallet 700–1000 ms. Kontrastförhållandena mellan grå- och vit hjärnsubstans är en viktig faktor för hur bra segmenteringen kan bli.
Projektet innehåller en volontärstudie omfattande 10 friska försökspersoner. Studien sker på en 3T Magnetom Trio (Siemens, Medical Solution, Erlangen, Tyskland) och innehåller även en jämförelse mellan en 12-och en 32 kanals Matrix huvudspole. En analys av histogrammen från bildinsamlingarna genomförs för att kvantifiera kontrast och klassificera vävnad. Bildernas diagnostiska kvalitet bedöms av en neuroradiolog.

Resultat
Kontrastskillnader på upp till 56 % kan hittas för de två parametrar som varieras i sekvensen. Det sammantaget bästa resultatet efter segmenteringen uppnås med en flippvinkel på 8 eller 9º och en inversionstid mellan 800 och 900 ms. Samtliga bilder tagna med dessa parameterinställningar bedömdes som godtagbara för diagnostik ur ett kliniskt perspektiv.

Konklusion
Inga andra studier om optimering av MPRAGE för volymetri som också innehåller en jämförelse mellan två olika flerkanalsspolar för ett 3T system har påträffats. Jämförelsen mellan 12-och 32 kanals mottagarspolarna visar att spolen med 32 kanaler ger en större variation av kontrasten mellan de olika vävnadstyperna när de parametrar som påverkar kontrasten justeras. Detta indikerar att spolen med 32 kanaler är i något större behov av en optimering än spolen med 12 kanaler.